Fewest Switches Adiabatic Surface Hopping As Applied to Vibrational Energy Relaxation†

Günter Käb‡

Max-Planck-Institut für Biophysikalische Chemie, Am Fassberg 11, D-37077 Göttingen, Germany

Received: August 15, 2005; In Final Form: January 12, 2006

In this contribution quantum/classical surface hopping methodology is applied to vibrational energy relaxation of a quantum oscillator in a classical heat bath. The model of a linearly damped (harmonic) oscillator is chosen which can be mapped onto the Brownian motion (Caldeira−Leggett) Hamiltonian. In the simulations Tully's fewest switches surface hopping scheme is adopted with inclusion of dephasing in the adiabatic basis using a simple decoherence algorithm. The results are compared to the predictions of a Redfield-type quantum master equation modeling using the classical heat bath force correlation function as input. Thereby a link is established between both types of quantum/classical approaches. Viewed from the latter perspective, surface hopping with dephasing may be interpreted as "on-the-fly" stochastic realization of a quantum/classical Pauli master equation.

1. Introduction

Because of the complexity of systems in condensed phase chemical and biological physics, a fully quantum dynamical description of processes is out of reach for these systems. While classical molecular dynamics of nuclear motion provides a versatile tool for investigation of large chemical and biomolecular systems,[1,2] many interesting situations require the inclusion of genuine quantum degrees of freedom,[2−4] most notably in photochemistry and photobiology,[5,6] or make the inclusion of quantum effects desirable for certain nuclear degrees of freedom (DoF), e.g., for proton-transfer reactions.[7,8] In this scenario a "divide and conquer" strategy seems to be the most fruitful avenue, where a usually small subsystem of interest is described quantum mechanically, while the majority of supposedly less important DoF, the environment or "heat bath", is treated by classical mechanics. The emerging methodology of mixed quantum/classical dynamics (QCMD) has been successfully applied to electronically nonadiabatic processes,[9−13] proton[7] and light atom (transfer) reactions,[8,14] and its origins date back to the early days of quantum dynamics.[15] Recently, the methodology has also been developed to study vibrational energy transfer in solution.[16−18]

Despite the progress being made, the field still reflects the influence of rather fundamental questions and issues. There is as yet no universally accepted quantum/classical method applicable to arbitrary systems or processes of interest. This is perhaps best illustrated by the multitude of different schemes adopted in the literature. While more traditional approaches propagate a time-dependent Schrödinger equation for the quantum subsystem self-consistently coupled to the classical dynamics of the environment,[4,9,19,20] more recent developments employ the density operator within a quantum/classical Liouville equation framework.[21−25]

At the heart of the quantum/classical dilemma is the notion of quantum open system dynamics and the emergent phenomenon of quantum decoherence,[26−28] i.e., the decay of coherences of the subsystem density matrix in a certain state basis depending on the system-environment interaction.[26,27] Quantum decoherence in a subsystem originates from genuine quantum system−bath correlations and is thus a priori absent from ad hoc quantum/classical treatments. Decoherence effects have been introduced by a number of researchers[25,29,30−32] (see also the references in ref 4), to provide a remedy to the problem of unphysical coherence in the simplest quantum/classical methods. The latter can be divided into two main categories, represented by the mean field Ehrenfest (mfE)[4,14] and trajectory surface hopping (SH, TSH) methods,[4,9] respectively. In both schemes the Schrödinger (or quantum Liouville) dynamics of the quantum subsystem is propagated fully coherently under the influence of a single classical trajectory of the environment, appropriately sampled from a classical or quasi-classical initial distribution (independent trajectory approximation). The backreaction on the classical dynamics, however, is treated differently. In the mfE method, the classical trajectory evolves on a mean field potential energy surface derived from the time-dependent expectation value of the system−bath interaction. In the SH method, the trajectory always evolves on one of the various instantaneous adiabatic surfaces (the "occupied" state), except for hops between surfaces accompanied by sudden momentum adjustments along the nonadiabatic coupling vector, accounting for quantum/classical energy conservation. The probability of hopping events is evaluated from the nonadiabatic coupling and the coherences in the adiabatic basis, and a fewest switches Monte Carlo hopping scheme is employed to maintain maximal consistency of the ensemble averaged subsystem density matrix populations and "occupied" state statistics.

While mfE is a fully coherent QCMD method, it suffers from the mean field backreaction which fails to reproduce the expected asymptotic statistical mixture of states for the quantum subsystem.[25,33,34] This is precisely the quantum/classical correlation problem which Tully's fewest switches TSH (TFS−TSH)[4,35] suggests to remedy by introducing hopping events between "occupied" adiabatic states, supposed to give the correct branching ratios implied by an asymptotic statistical mixture. Often, however, a discrepancy between (or inconsistency of) ensemble averaged density matrix and "occupied" state populations is observed. This is commonly (or most oftenly) associated with "frustrated hops"[14,25] or "classically forbidden transi-

† Part of the special issue "Jürgen Troe Festschrift".

‡ E-mail: gkaeb@gwdg.de. Telephone: +49 (0)551/201-1256. Fax: +49 (0)551/201-1006.

10.1021/jp054577k CCC: $33.50
Published on Web 02/16/2006

tions",[4,11] where the nonadiabatic coupling and adiabatic coherences suggest hopping to an excited state, while there is not enough kinetic energy available in the classical subsystem, so the hop must be rejected. There appears to be no rigorous way to handle this problem within a quantum/classical framework, and different interpretations and strategies have been proposed,[4,11,36−9] also in connection with mean field Ehrenfest[14,20,40] and the decoherence issue.[25,32,39] We suggest that the problem of "frustrated hopping" is connected, in part, to the absence of decoherence/dephasing from TSH: The quantum subsystem state vector (or density operator) is propagated coherently throughout, even though hops between adiabatic surfaces occur. Thus, during single trajectory SH evolution, the currently "occupied" adiabatic state may acquire an associated density matrix population significantly smaller than unity and large coherences with other states (especially states of higher energy), as will be demonstrated. As a result, transition probabilities may become large, while a large fraction of suggested hops must be rejected due to energy conservation restrictions. It seems hard to believe that this inconsistency is simply removed by ensemble averaging, given the assumed validity of the independent trajectory approximation. However, as will be illustrated below, the statistics of "frustrated hopping" is also connected to quantum detailed balance,[41] i.e., the statistical ratio of up and down transitions between energy states. Thus, it seems natural to expect that even in the most consistent TSH scheme some fraction of "frustrated hops" must remain, so there is some truth in the phenomenon of rejected hopping.

The suggested detailed balance related "frustrated hopping" brings us to our final introductory point, the question of asymptotic thermal equilibrium for the quantum subsystem immersed in a classical heat bath. In a recent study, it has been demonstrated that mean field Ehrenfest QCMD, applied to a quantum oscillator interacting with a classical heat bath,[33,34] gives (when it works reasonably) at best a quasi-classical asymptotic thermal equilibrium. This can be rationalized in terms of a classical dynamical correlation between quantum and classical subsystems. The same type of asymptotic analysis is also of interest for SH, and one of our aims in the present work. While it is expected that TSH entails a quantum statistical equilibrium for the subsystem of interest,[41] we will also be concerned with the rate of approach to equilibrium. Moreover, we will see that the maintenance of quantum detailed balance in surface hopping simulations may depend on whether a mechanism of dephasing (or decoherence in the energy basis) is invoked.

Given our above criticism, we take a rather modest attitude and apply fewest switches SH to a deceptively simple model system, which nevertheless poses a considerable challenge to surface hopping,[42] a harmonic oscillator bilinearly coupled to a heat bath of harmonic oscillators. To achieve consistency of density matrix and "occupied" state populations already at the single-trajectory level, we introduce a simple decoherence algorithm which basically consists of associating with each successful hopping event a "collapse" of the vibrational wave packet onto the new "occupied" adiabatic state. In view of our later discussion, this is, however, not to be understood in terms of a measurement-like interaction between the quantum subsystem and its environment. Implicitly we assume that the vibrationally nonadiabatic coupling is in the perturbative regime, such that the adiabatic coherences should remain small and the adiabatic populations vary slowly.

At this point, we add some remarks on the notions of decoherence and dephasing, to avoid confusion. As has already become apparent, we use the latter two terms interchangeably. While the term dephasing seems to most oftenly be associated with the loss of phase coherence between energy states (most notably in spectroscopy), leading for instance to decay of the displacement and momentum expectation values of a damped oscillator, the term decoherence, in its more general form, applies to the decay of coherences from a subsystem density matrix, in whatever basis. Sometimes the notion of dephasing is also used in this manner. Since we are referring, mainly, to decoherence in the (adiabatic) energy basis, it may be understood as equivalent to dephasing in the above sense. Later, we will need to distinguish between different origins of dephasing, including pure dephasing (due to some type of random frequency modulation), dephasing due to energy/population relaxation (damping of oscillations), and genuine quantum decoherence arising from quantum system−bath entanglement.[26,27] Thereby, we deliberately subsume the distinct phenomenon of quantum decoherence under the more general heading of "decoherence/dephasing" ("loss of phase coherence"), although this may not seem acceptable to all readers, and the term decoherence, in its more narrow sense, is even understood as quantum decoherence.[26,27] A detailed discussion of decoherence/dephasing mechanisms in quantum/classical dynamics simulations will be given in the Results.

Our paper is organized as follows. In section 2, fewest switches adiabatic surface hopping is briefly reviewed. The Brownian motion model, used in the simulations, is introduced, and the second order Redfield master equation applied to this model. In particular, the secular limit of the Redfield master equation and its quantum/classical implementation form the basis for the analysis of trajectory surface hopping simulations presented in section 3, where Tully's original TFS−SH method and our modified "hopping with complete dephasing" version are compared. This section also examines different origins of dephasing as to their relevance for the model situation considered. Section 4 concludes.

2. Theory

2.1. Fewest Switches Adiabatic Surface Hopping. For completeness, we give here a short review of Tully's fewest switches SH (TFS−SH).[4,9,35] For a total Hamiltonian of the general type

$$\hat{H} = \hat{H}_S(q,p) + \hat{V}(q,\mathbf{Q}) + \hat{H}_B(\mathbf{Q},\mathbf{P})$$

$$\hat{H}_S(q,p) = \frac{\hat{p}^2}{2\mu} + \hat{V}_S(q)$$

$$\hat{H}_B(\mathbf{Q},\mathbf{P}) = \sum_i \frac{\hat{P}_i^2}{2m_i} + \hat{V}_B(\mathbf{Q}) \qquad (1)$$

where $\mathbf{Q} \equiv \{Q_i\}$ and $\mathbf{P} \equiv \{P_i\}$, or collectively $\mathbf{X} \equiv (\mathbf{Q}, \mathbf{P})$, the TSH quantum/classical equations of motion take the form

$$\frac{\mathrm{d}}{\mathrm{d}t}|\Psi_S(t)\rangle = -\frac{i}{\hbar}\{\hat{H}_S + \hat{V}[q;\mathbf{Q}(t)]\}|\Psi_S(t)\rangle \equiv -\frac{i}{\hbar}\hat{H}_q[q;\mathbf{Q}(t)]|\Psi_S(t)\rangle$$

$$\dot{\mathbf{Q}}(t) = \frac{\partial H_B(\mathbf{X})}{\partial \mathbf{P}}\Big|_{\mathbf{X}=\mathbf{X}(t)}$$

$$\dot{\mathbf{P}}(t) = -\frac{\partial H_B(\mathbf{X})}{\partial \mathbf{Q}}\Big|_{\mathbf{X}=\mathbf{X}(t)} - \frac{\partial \epsilon_m[\mathbf{Q}]}{\partial \mathbf{Q}}\Big|_{\mathbf{Q}=\mathbf{Q}(t)} \qquad (2)$$

where $\hat{H}_S$ and $\hat{H}_B$ denote the system and bath Hamiltonian, respectively, and $\epsilon_m[\mathbf{Q}(t)]$ is the energy eigenvalue associated with the currently occupied instantaneous adiabatic state, $\hat{H}_q[q; \mathbf{Q}(t)]\,|\chi_m[\mathbf{Q}(t)]\rangle = \epsilon_m[\mathbf{Q}(t)]\,|\chi_m[\mathbf{Q}(t)]\rangle$. Thus, the quantum subsystem evolves coherently, while the classical trajectory of the environmental degrees of freedom (DoF) is confined to a single adiabatic potential energy surface. The time-dependent Schrödinger eq 2 can be integrated using any suitable bases and unitary propagation scheme. In the simulations presented a modified PICKAPACK algorithm[43−45] was used. When the quantum state vector is projected onto the adiabatic basis, $a_m[\mathbf{Q}(t);t] = \langle\chi_m[\mathbf{Q}(t)]|\Psi_S(t)\rangle$, the amplitude equations of motion read

$$\frac{\mathrm{d}}{\mathrm{d}t}\,a_m[\mathbf{Q}(t);t] = -i\omega_m[\mathbf{Q}(t)]\;a_m[\mathbf{Q}(t);t] - \sum_{n\neq m}\{\mathbf{d}_{mn}[\mathbf{Q}(t)]\cdot\dot{\mathbf{Q}}(t)\}a_n[\mathbf{Q}(t);t] \quad (3)$$

where $\mathbf{d}_{mn}[\mathbf{Q}(t)]$ is the nonadiabatic coupling vector with components[4]

$$\begin{aligned} d^{(i)}_{mn}[\mathbf{Q}(t)] &= \langle\chi_m[\mathbf{Q}(t)]|\nabla_i\,\chi_n[\mathbf{Q}(t)]\rangle \\ &= -\frac{\langle\chi_m[\mathbf{Q}(t)]|\nabla_i\,\hat{H}_q[q;\mathbf{Q}(t)]|\chi_n[\mathbf{Q}(t)]\rangle}{\epsilon_m[\mathbf{Q}(t)] - \epsilon_n[\mathbf{Q}(t)]} \\ &= -\{d^{(i)}_{nm}[\mathbf{Q}(t)]\}^* \\ d^{(i)}_{mm}[\mathbf{Q}(t)] &= 0 \end{aligned} \quad (4)$$

Thus, the rate of change of the currently occupied adiabatic state population becomes

$$\frac{\mathrm{d}}{\mathrm{d}t}\,\rho_{mm}[\mathbf{Q}(t);t] = -2\sum_{n\neq m}\mathrm{Re}\{\mathbf{d}_{mn}[\mathbf{Q}(t)]\cdot\dot{\mathbf{Q}}(t)\;\rho_{nm}[\mathbf{Q}(t);t]\} \quad (5)$$

with $\rho_{mn}[\mathbf{Q}(t);t] = a_m[\mathbf{Q}(t);t]a^*_n[\mathbf{Q}(t);t]$. In the fewest switches implementation[35] the transition probability $t_{m\to n}(t;\delta t)$ out of state m into state n is evaluated to

$$\begin{aligned} t_{m\to n}(t;\delta t) &= -\frac{\mathrm{d}}{\mathrm{d}t}\,\rho_{mm}[\mathbf{Q}(t);t]|_n\delta t \\ &= +2\;\mathrm{Re}\{\mathbf{d}_{mn}[\mathbf{Q}(t)]\cdot\dot{\mathbf{Q}}(t)\;\rho_{nm}[\mathbf{Q}(t);t]\}\delta t \end{aligned} \quad (6)$$

with δt being the time increment used in the simulation (chosen suitably small), and the associated hopping probability $p_{m\to n}(t;\delta t)$ (probability of escape into state n) is calculated as

$$p_{m\to n}(t;\delta t) = \mathrm{max}\left\{0, \frac{t_{m\to n}(t;\delta t)}{\rho_{mm}[\mathbf{Q}(t);t]}\right\} \quad (7)$$

In this way, fewest switches SH ensures that only escape events from state m are sampled during coherent evolution of the quantum subsystem. In every time step, a uniformly distributed random number $\xi \in [0, 1]$ is generated, where the condition

$$\sum_{k=1}^{n-1} p_{m\to k} < \xi \leq \sum_{k=1}^{n} p_{m\to k}(t;\delta t) \quad (8)$$

suggests a hop to the new adiabatic state n. In order for the hop to occur, energy conservation must be fulfilled, while the momentum is adjusted along the nonadiabatic coupling vector $\mathbf{d}_{mn}$,[11]

$$\mathbf{P}_n = \mathbf{P}_m + \sigma\,\mathbf{e}_{mn} \qquad \mathbf{e}_{mn} = \frac{\mathbf{d}_{mn}}{\sqrt{\mathbf{d}_{mn}\cdot\mathbf{d}_{mn}}} \quad (9)$$

where $\mathbf{P}_m$ and $\mathbf{P}_n$ are the (mass-weighted) momentum vectors before and after the hop, respectively, and $\mathbf{e}_{mn}$ the unit vector along $\mathbf{d}_{mn}$. Equation 9, together with energy conservation $K_n + \epsilon_n[\mathbf{Q}(t)] = K_m + \epsilon_m[\mathbf{Q}(t)]$, yields a quadratic equation for σ and thus

$$\mathbf{P}_n = \mathbf{P}_m - (\mathbf{P}_m\cdot\mathbf{e}_{mn})\mathbf{e}_{mn} \pm \sqrt{(\mathbf{P}_m\cdot\mathbf{e}_{mn})^2 - 2\Delta\epsilon_{nm}[\mathbf{Q}(t)]}\;\mathbf{e}_{mn} \quad (10)$$

which poses the requirement $(\mathbf{P}_m\cdot\mathbf{e}_{mn})^2 \geq 2\Delta\epsilon_{nm}[\mathbf{Q}(t)]$; i.e., for $\epsilon_n[\mathbf{Q}(t)] > \epsilon_m[\mathbf{Q}(t)]$ enough kinetic energy along $\mathbf{d}_{mn}$ must be available, otherwise hopping to a higher energy state must be rejected. The latter case corresponds to the "frustrated hopping" situation mentioned above. For a successful hop the $\pm$ sign may be chosen such as to minimize the momentum shift.

Before closing this subsection, we mention that TFS−TSH may be mapped onto a Markovian Pauli master equation for the adiabatic state populations $p_m(t)$

$$\frac{\mathrm{d}}{\mathrm{d}t}\,p_m(t) = -p_m(t)\sum_{n\neq m} w_{m\to n} + \sum_{n\neq m} p_n(t)\;w_{n\to m} \quad (11)$$

where the transition rates $w_{m\to n}$ can be identified with $\langle p_{m\to n}(t;\delta t)\rangle/\delta t$, i.e., $w_{m\to n}$ is the ensemble averaged rate of escape from state m to state n, sampled during a coherent evolution of the quantum subsystem density matrix while the classical environmental trajectory is confined to the adiabatic surface of state m. For reasons of consistency (possibly already on the single-trajectory level), during coherent sampling of $\langle p_{m\to n}(t;\delta t)\rangle$ the adiabatic population $\rho_{mm}[\mathbf{Q}(t);t]$ should remain close to unity (or at least >0.5) and the adiabatic coherences small, such that the nonadiabatic coupling may be considered as a perturbation.

Even if this is initially the case, immediately after successful hopping to a new state n the population typically lags behind, the dominant population is still $\rho_{mm}[\mathbf{Q}(t);t]$. For a consistent sampling of $\langle p_{n\to n'}(t;\delta t)\rangle$ the dominant population should now be $\rho_{nn}[\mathbf{Q}(t);t]$. This suggests resetting the state vector to $|\chi_n[\mathbf{Q}(t)]\rangle$ during hopping, i.e., an apparent "collapse" of the coherent wave packet onto adiabatic state n. This line of reasoning is also consistent with a quantum master equation in the secular limit,[46] where the rate of (local) population relaxation sets a lower bound to dephasing (see below). When fewest switches TSH is interpreted and implemented in this way, it may be viewed as an "on-the-fly" stochastic realization of a Pauli master equation (eq 11), with the transition rates a priori unknown. The sampling of rate coefficients (rates of escape) $w_{m\to n}$ by way of eq 7 starting from the respective pure adiabatic states m then corresponds to a flux-over-population method.[47]

2.2. Model Hamiltonian and Dissipative Subsystem Dynamics. In the present study, we consider the simple system of a harmonic oscillator linearly perturbed by the interaction $V_{SB} = -qF$ with a heat bath, where F is the force excerted on the relevant subsystem by the many bath DoF. This situation may be mapped onto the model of one-dimensional motion in a

potential $V_S(q)$, bilinearly coupled to a bath of harmonic oscillators

$$\hat{H} = \frac{\hat{p}^2}{2\mu} + \hat{V}_S(q) + \sum_l \left\{ \frac{\hat{P}_l^2}{2} + \frac{\omega_l^2}{2}\left(\hat{Q}_l - \frac{g_l}{\omega_l^2}\hat{q}\right)^2 \right\} \quad (12)$$

known as the Brownian motion or Caldeira−Leggett Hamiltonian.[47−50] It provides, for instance, the basis for a rigorous microscopic formulation of the generalized Langevin equation (GLE)[48,51,52]

$$\frac{\mathrm{d}}{\mathrm{d}t} p(t) = -\frac{\mathrm{d}V_S(q)}{\mathrm{d}q} - \int_0^t \mathrm{d}s\, \gamma(t-s)\, p(s) + \delta F(t) \quad (13)$$

in classical and quantum dynamics, where $\gamma(t)$ is the friction kernel and $\delta F(t)$ a fluctuating force, with the statistical properties[48,53]

$$\langle \delta F(t) \rangle = 0$$

$$C(t) \equiv \langle \delta\hat{F}(t)\delta\hat{F}(0)\rangle = \sum_l \frac{\hbar g_l^2}{2\omega_l}\{(\bar{n}_l + 1)\, \mathrm{e}^{-i\omega_l t} + \bar{n}_l\, \mathrm{e}^{+i\omega_l t}\}$$

$$C_{cl}(t) \equiv \langle \delta F(t)\delta F(0)\rangle = k_B T \sum_l \frac{g_l^2}{\omega_l^2} \cos\omega_l t \equiv \mu k_B T \gamma(t) \quad (14)$$

where in the quantum case $\bar{n}_l = \langle \hat{a}_l^\dagger \hat{a}_l \rangle$ is the mean occupation number of the lth bath oscillator at thermal equilibrium.

For small system−bath interaction $\hat{V}_{SB} = -\hat{q}\sum_l g_l \hat{Q}_l$ a second-order generalized quantum master equation may be obtained,[53] which in the limit of short bath correlation time (on the system's time scale) may be written in a Markovian (time local) Redfield-type form,[46,53,54]

$$\frac{\mathrm{d}}{\mathrm{d}t}\hat{\rho}_S(t) = -\frac{i}{\hbar}[\hat{H}_S, \hat{\rho}_S(t)] - \frac{1}{\hbar^2}\{[\hat{q}, \hat{\Lambda}\,\hat{\rho}_S(t)] - [\hat{q}, \hat{\rho}_S(t)\,\hat{\Lambda}^\dagger]\} \quad (15)$$

where the dissipators $\hat{\Lambda} = \int_0^\infty \mathrm{d}t\, C(t)\, \hat{q}_S(-t)$ and $\hat{\Lambda}^\dagger = \int_0^\infty \mathrm{d}t\, C^*(t)\, \hat{q}_S(-t)$ contain the system Heisenberg operator $\hat{q}(t)$ propagated backward in time under the system Hamiltonian $\hat{H}_S$. By invoking the secular limit[46,53] the Redfield master equation may be further simplified, where the populations $\rho_{nn}(t)$ of system energy eigenstates, $\hat{H}_S|n\rangle = \epsilon_n|n\rangle$, are decoupled from the coherences $\rho_{mn}(t)$ and evolve according to a Pauli master equation (eq 11) with transition rates

$$w_{m\to n} = \frac{|q_{mn}|^2}{\hbar^2}\int_{-\infty}^{+\infty} \mathrm{d}t\, C(t)\, \mathrm{e}^{-i\omega_{nm}t} \quad (16)$$

The detailed balance relationship between $w_{m\to n}$ and $w_{n\to m}$ is embodied in the properties of the correlation spectrum[53]

$$\hat{C}(+\omega) = \int_{-\infty}^{+\infty} \mathrm{d}t\, C(t)\, \mathrm{e}^{-i\omega t} = \mu\,\hbar\omega\bar{n}(\omega, T)\,\hat{\gamma}(\omega)$$

$$\hat{C}(-\omega) = \int_{-\infty}^{+\infty} \mathrm{d}t\, C(t)\, \mathrm{e}^{+i\omega t} = \int_{-\infty}^{+\infty} \mathrm{d}t\, C^*(t)\, \mathrm{e}^{-i\omega t} = \mu\,\hbar\omega\{\bar{n}(\omega, T) + 1\}\hat{\gamma}(\omega) \quad (17)$$

giving $\hat{C}(-\omega) = e^{\beta\hbar\omega}\hat{C}(+\omega)$. For the damped harmonic oscillator only single-quantum transitions are allowed

$$w_{n\to n+1} = \frac{\hat{\gamma}(\omega_0)}{2}\,\bar{n}(\omega_0)\,(n+1)$$

$$w_{n\to n-1} = \frac{\hat{\gamma}(\omega_0)}{2}\,\{\bar{n}(\omega_0) + 1\}n \quad (18)$$

and the overall energy (occupation number) relaxation is exponential with rate constant $\bar{w} = \hat{\gamma}(\omega_0)/2$, the half-sided cosine transform of the friction kernel. For the Brownian motion model (eqs 12 and 13) quantum and classical rates of energy relaxation are equal, $\bar{w} = \bar{w}_{cl}$. The evolution of coherences in the secular limit is characterized by relaxation-induced dephasing and a (usually small) frequency shift

$$\frac{\mathrm{d}}{\mathrm{d}t}\rho_{mn}(t) = -i\{\omega_{mn} + \delta\omega_{mn}\}\rho_{mn}(t) - \frac{1}{\tau_{mn}}\rho_{mn}(t)$$

$$\frac{1}{\tau_{mn}} = \frac{1}{2}\{\sum_{k\neq m} w_{m\to k} + \sum_{k\neq n} w_{n\to k}\} \quad (19)$$

Thus, the rates for local population (energy) relaxation define a maximum time scale for dephasing (decoherence in the energy basis). The case of adiabatic coherences is analoguous. This is one of our motivations for introducing the simple decoherence algorithm into TFS−SH, as mentioned in the previous subsection. Although we deal here with situations of weak dissipative system−bath coupling, the reasoning is more general and also applies to weak vibronic interaction between potential energy surfaces.

Before closing this subsection, we briefly discuss, for later reference, one particular quantum/classical modeling approach to vibrational energy relaxation within the framework of Redfield theory. It exploits the fact that equilibrium quantum time correlation functions have the property[53] $C^*(t) = C(-t)$, and therefore can always be written as a sum of time-symmetric and -antisymmetric contributions, $C(t) = C_+(t) + C_-(t)$ and $C^*(t) = C_+(t) - C_-(t)$. The Fourier transforms of symmetric and antisymmetric parts are related to $\hat{C}(\omega)$ via

$$\hat{C}_+(\omega) = \frac{1}{2}\{1 + \mathrm{e}^{\beta\hbar\omega}\}\hat{C}(\omega) \quad \hat{C}_-(\omega) = \frac{1}{2}\{1 - \mathrm{e}^{\beta\hbar\omega}\}\hat{C}(\omega) \quad (20)$$

For general condensed phase situations, the quantum force correlation function is unknown, which suggests making use of its classical counterpart via the correspondence $C_+(t) \leftrightarrow C_{cl}(t)$, i.e., invoking the high-temperature limit for $C_+(t)$.[33,55,56] The transition rates (eq 16) then read

$$w_{m\to n} = \frac{|q_{mn}|^2}{\hbar^2}\,\frac{2}{1 + \mathrm{e}^{\beta\hbar\omega_{nm}}}\,\hat{C}_{cl}(\omega_{nm}) \quad (21)$$

and for the damped harmonic oscillator

$$w_{n\to n+1} = \frac{(n+1)}{2\hbar\omega_0}\,\frac{2k_BT\hat{\gamma}(\omega_0)}{1 + \mathrm{e}^{\beta\hbar\omega_0}} \equiv \frac{2k_BT}{\hbar\omega_0(2\bar{n}+1)}\,\frac{\hat{\gamma}(\omega_0)}{2}\,\bar{n}(n+1)$$

$$w_{n\to n-1} = \frac{n}{2\hbar\omega_0}\,\frac{2k_BT\hat{\gamma}(\omega_0)}{1 + \mathrm{e}^{-\beta\hbar\omega_0}} \equiv \frac{2k_BT}{\hbar\omega_0(2\bar{n}+1)}\,\frac{\hat{\gamma}(\omega_0)}{2}\,(\bar{n}+1)n \quad (22)$$

The overall decay of energy (mean occupation number) is therefore

$$\frac{\mathrm{d}}{\mathrm{d}t}\langle\hat{n}\rangle = -\bar{w}_{qc}\{\langle\hat{n}\rangle - \bar{n}(\omega_0)\} \qquad \bar{w}_{qc} = \frac{2k_\mathrm{B}T}{\hbar\omega_0(2\bar{n}+1)}\,\bar{w}_{cl} \tag{23}$$

where the prefactor ($f(\omega_0,T) \leq 1$), relating $\bar{w}_{qc}$ and $\bar{w}_{cl} = \hat{\gamma}(\omega_0)/2$ through $\bar{w}_{qc} = f(\omega_0,T)\,\bar{w}_{cl}$, arises from employing the correspondence $C_+(t) \cong C_{cl}(t)$ in combination with quantum detailed balance, eqs 17 and 20. As will be demonstrated below, this is the result obtained from TFS−TSH simulations, with inclusion of dephasing, based on the Brownian motion Hamiltonian.

3. Results and Discussion

3.1. Model Parameterization and Simulations. For the Brownian motion Hamiltonian, eq 12, applied to the damped harmonic oscillator (HO) the coherent TFS−SH equations of motion, eq 2, read

$$\frac{\mathrm{d}}{\mathrm{d}t}|\Psi_\mathrm{S}(t)\rangle = -\frac{i}{\hbar}\{\hat{H}_\mathrm{solv} - \hat{q}\sum_l g_l Q_l(t)\}|\Psi_\mathrm{S}(t)\rangle$$

$$\hat{H}_\mathrm{solv} = \hbar\omega_0\left\{\hat{n}+\frac{1}{2}\right\} + \frac{1}{2}\sum_l \frac{g_l^{\,2}}{\omega_l^{\,2}}\,\hat{q}^2$$

$$\dot{P}_l(t) = \ddot{Q}_l(t) = -\omega_l^{\,2}\,Q_l(t) + g_l\,q_{mm}[\mathbf{Q}(t)] \tag{24}$$

In the simulations, an ohmic spectral density of bath oscillators[53,57]

$$J(\omega) \equiv \frac{\pi}{2}\sum_l \frac{g_l^{\,2}}{\omega_l}\,\delta(\omega-\omega_l) = \mu\gamma\omega\;\mathrm{e}^{-\omega/\omega_c} \tag{25}$$

with exponential cutoff has been assumed, where the force correlation spectrum ($\omega \geq 0$) is given by

$$\hat{C}(\omega) = 2\hbar\,J(\omega)\,\bar{n}(\omega,T) \equiv 2\mu\gamma\,\hbar\omega\bar{n}(\omega,T)\,\mathrm{e}^{-\omega/\omega_c}$$

$$\hat{C}_{cl}(\omega) = 2k_\mathrm{B}T\frac{J(\omega)}{\omega} \equiv 2\mu\gamma\,k_\mathrm{B}T\,\mathrm{e}^{-\omega/\omega_c} \tag{26}$$

For the system oscillator a harmonic frequency of $\omega_0/2\pi = 250$ cm^{-1} has been chosen, and the bath spectral density adjusted such that $\hat{\gamma}(\omega_0)/2 \cong 0.2$ ps^{-1} ($\gamma = 2.0$ ps^{-1}, $\omega_c/2\pi = 108.574$ cm^{-1}), and discretized using 2000 classical oscillators in the range $0-10\;\omega_c$. The choice of a rather low-frequency system oscillator helps avoiding small integration steps, while classical and quantum equilibrium statistics are still distinguishable.

An ensemble of 1000 independent quantum/classical nonequilibrium trajectories has been generated, starting from a mean energy of $\langle\hat{n}\rangle_0 = 5$ vibrational quanta and a classical canonical distribution of bath initial conditions at $T = 300$ K, in the presence of the quantum subsystem (see below). Each trajectory was initialized with its own random seed with respect to the selection of bath oscillator initial conditions and the surface hopping algorithm, and run for up to 15 ps. For each random initial state of the heat bath, only a single sequence of surface hops was performed, instead of trying to converge both the surface hopping statistics for every single bath initial condition and the canonical sampling of the latter. We note that this may be considered a severe deviation from the TFS−SH protocol, where a bunch of different SH trajectories (with different random seeds) should be generated from the same (random) classical bath initial condition. Moreover, an exhaustive sampling of SH statistics for each given classical initial condition would require enough trajectories such that each possible SH branching situation $m \rightarrow \{n\}$ at time $t \in [t_0, t_\mathrm{max}]$ is visited more than once. In practice, the difference between our present TFS−TSH protocol and the general scheme may be assumed to vanish, provided that the initial conditions of the classical bath force are sampled sufficiently densely. Our experience with running several SH trajectories per classical initial condition, while keeping the (sufficiently large) total number of trajectories fixed (reducing the number of classical initial conditions), seems to suggest that this is the case. Thus, the above more simple TFS−SH protocol in principle does not reduce the computational effort (total number of trajectories at assumed convergence). For the present model, at least, it rather appears as a matter of algorithmic convenience. In general, of course, it is necessary to keep an eye on these matters.

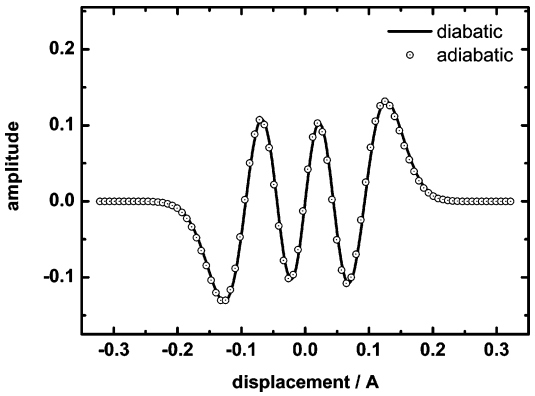

Figure 1. Initial quantum state in position space (*diabatic* state). The corresponding adiabatic wave function is only slightly shifted in origin, due to bath initial conditions.

The initial wave function has been chosen to be an eigenstate $|n_0\rangle = |5\rangle$ of $\hat{H}_\mathrm{S} = \hbar\omega_0\hat{n}$ (diabatic state), which differs very little from the corresponding adiabatic state (Figure 1), and the initial state of each bath oscillator is chosen from

$$\rho(Q_l,P_l) = Z^{-1}\exp\left\{-\frac{P_l^{\,2}}{2k_\mathrm{B}T} - \frac{\omega_l^{\,2}}{2k_\mathrm{B}T}\left(Q_l - \frac{g_l}{\omega_l^{\,2}}\langle\hat{q}\rangle_0\right)^2\right\} \tag{27}$$

i.e. *mean field correlated*[34] instead of *factorized* quantum/classical initial conditions. Thereby, problems arising from factorized initial conditions[52,58] are avoided in general, although for the present special case of a damped HO, with diabatic initial state, $\langle\hat{q}\rangle_0 = 0$.

The heat capacity $C_V = 2000k_B$ of the classical bath ensures that the rise of bath temperature is kept below 1 K. Also, by choosing a suitably large heat bath, it is made sure that recurrences of the friction kernel $\gamma(t)$ (eqs 13 and 14) do not show up within the time-window considered, and the dynamics of the quantum subsystem appears as irreversible.

The coherent quantum/classical equations of motion (eqs 2 and 24) were solved numerically using a symplectic quantum/classical symmetric split propagator as described elsewhere,[34] using a combination of $\hat{H}_\mathrm{S}$ ($\hat{H}_\mathrm{solv}$) eigenstate and position space (sinc-DVR) representations. In the case of rejected hops, instead of reversing the classical momenta along the nonadiabatic coupling vector[36] we have chosen to continue the coherent quantum/classical propagation as if no hop had been suggested.[11,37,38]

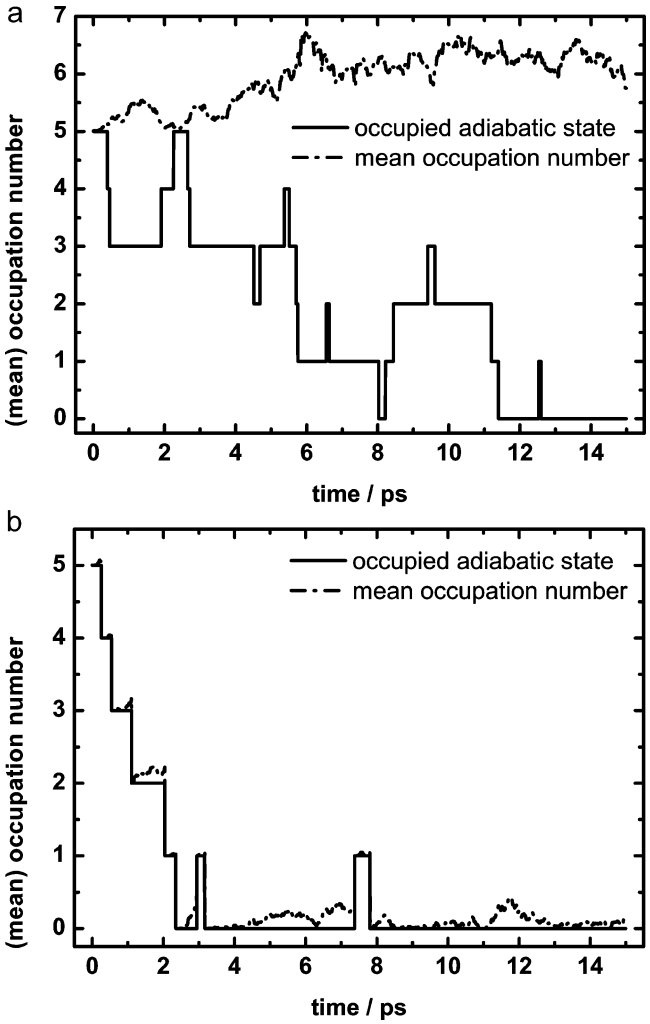

Figure 2. Single trajectory time evolution of the occupied adiabatic state $m(t)$ (adiabatic occupation number) and the mean adiabatic occupation number $\langle \hat{n}_{ad} \rangle_t$, for (a) Tully's original and (b) our modified TFS−TSH.

3.2. Simulation Results. 3.2.1. Energy Relaxation. In Figures 2 and 3 the single-trajectory and ensemble-averaged energy relaxation behavior is illustrated for both the original TFS−SH scheme (no dephasing) and our modified version including dephasing (decoherence in the adiabatic energy basis). The performance of Tully's original scheme for vibrational energy relaxation, in particular its failure to reproduce an asymptotic quantum statistical equilibrium for the subsystem oscillator, motivates our introduction of decoherence.

For the sake of clarity and definiteness, we distinguish between the expectation value $\langle \hat{n}_{ad} \rangle = \langle \Psi_S(t) | \hat{n}_{ad} | \Psi_S(t) \rangle$ of the number operator $\hat{n}_{ad} = \hat{n}_{ad}[\mathbf{Q}(t)]$ (in the adiabatic basis, see eq 31 below) and the associated eigenvalue $m = \langle m | \hat{n}_{ad} | m \rangle$, where $|m\rangle = |\chi_m[\mathbf{Q}(t)]\rangle$ is an instantaneous adiabatic vibrational state of the linearly perturbed quantum harmonic oscillator (specifically, the occupied state), and the adiabatic state index m corresponds to the vibrationally adiabatic quantum number, i.e., the number of energy quanta (occupation number) of the adiabatically displaced harmonic oscillator (see eq 31 below).

For Tully's original TFS−SH scheme, in Figure 2a the evolution of the assigned occupied adiabatic state $m = \langle m | \hat{n}_{ad} | m \rangle$ along a single TSH trajectory is shown and compared to the mean occupation number $\langle \hat{n}_{ad} \rangle$ in the adiabatic basis (the shifted HO basis), as calculated from the quantum amplitudes. As is clearly visible, due to fully coherent propagation of quantum amplitudes the classical heat bath tends to drive the quantum subsystem to a higher mean energy ($\langle \hat{n}_{ad} \rangle$), a behavior which is similar to mean field Ehrenfest dynamics starting from an (excited) energy eigenstate.[33,34] In particular, the mean occupa-

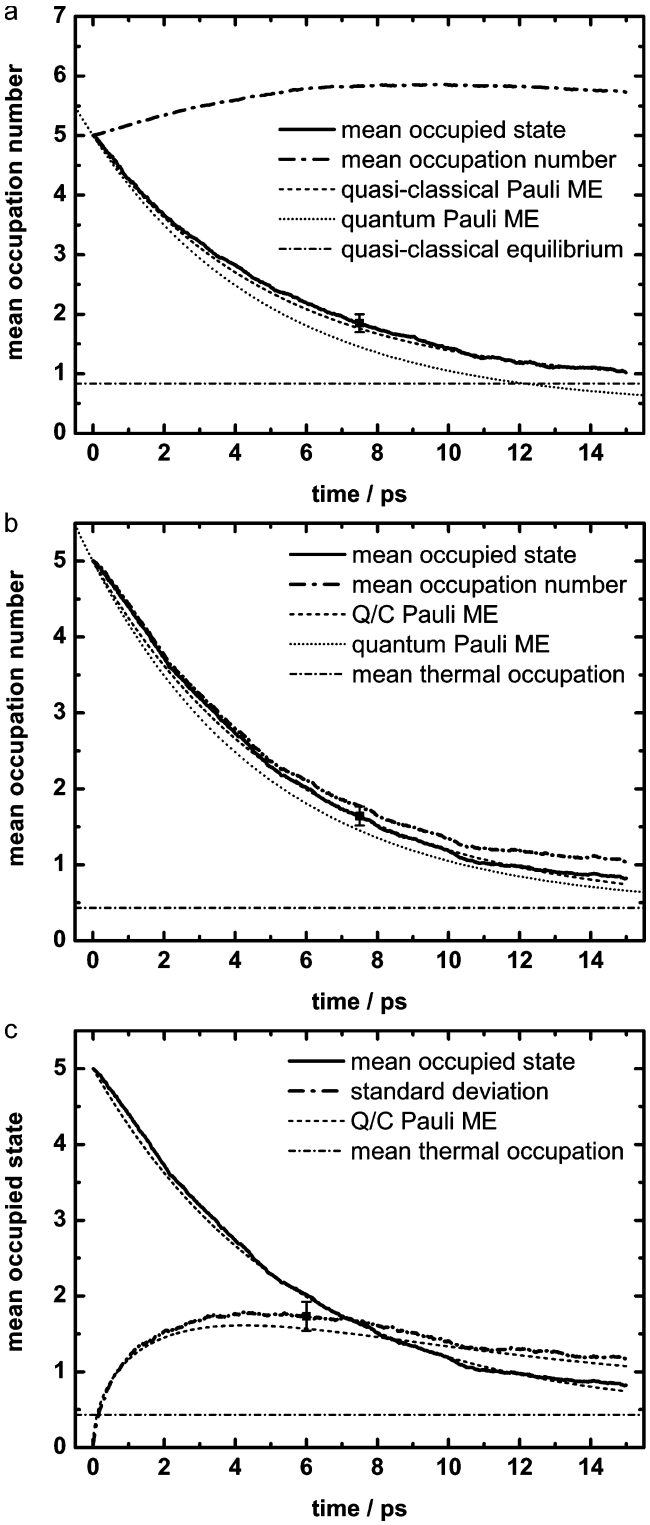

Figure 3. Ensemble averaged time evolution of mean occupied state and mean occupation number: (a) for the original TFS−SH, compared to the quasi-classical PME and quantum PME predictions; (b) for our modified TFS−SH, compared to the quantum/classical PME and quantum PME predictions. (c) Ensemble averaged time evolution of mean occupied state and standard deviation, for our modified TFS−SH, compared to the quantum/classical PME prediction. Numerical data points with error bars serve to indicate the respective overall statistical uncertainties (<10%).

tion number $\langle \hat{n}_{ad} \rangle$ never falls below its value at time zero. This is a general result, which is due to the quantum number dependence of the nonadiabatic coupling vector, where $\mathbf{d}_{m,m+1} \propto \sqrt{m+1}$ and $\mathbf{d}_{m,m-1} \propto \sqrt{m}$ in the present case (see the section below on a statistical treatment). In contrast, the occupied state index m seems to evolve toward states of lower energy, as expected for a subsystem coupled to a thermal reservoir. As a result, $\langle \hat{n}_{ad} \rangle \geq m$ for all times. The large discrepancy between m and $\langle \hat{n}_{ad} \rangle \geq m$ implies that, except at $t = 0$, the occupied state m is—for almost all times—not the dominant state in the expansion of the quantum state vector $|\Psi_S(t)\rangle$. It also implies that the quantum coherences $\rho_{mn}(t) = a_m(t)a_n^*(t)$ involving the currently occupied adiabatic state m are particularly large for higher excited states $n > m$ and thus favor transitions to these energy levels, provided enough energy is available in the classical subsystem. Transitions to lower levels $n < m$ are possible only to the extent that the respective states are contained in the expansion of $|\Psi_S(t)\rangle$.

Upon ensemble averaging the energy relaxation behavior as shown in Figure 3a is obtained. Again, $\langle \hat{n}_{ad} \rangle \geq \langle m \rangle$ as in the single-trajectory case. While the mean occupied adiabatic state $\langle m \rangle$ smoothly relaxes toward lower energies $\hbar\omega_0\langle m \rangle$ (in fact exponentially to a good approximation), the mean occupation number $\langle \hat{n}_{ad} \rangle$ evolves toward higher energies $\hbar\omega_0\langle \hat{n}_{ad} \rangle_t > \hbar\omega_0 \langle \hat{n}_{ad} \rangle_0$. The latter behavior again very closely resembles the results obtained with the mean field Ehrenfest scheme, when starting from an excited energy eigenstate,[34] where $\hbar\omega_0\langle \hat{n} \rangle_t \rightarrow \hbar\omega_0\langle \hat{n} \rangle_0 + k_BT$ is obtained. A detailed analysis is skipped here, because the evolution of $\langle \hat{n}_{ad} \rangle$ is not of physical relevance (at least not explicitly). In Figure 3a is also shown the decay of mean occupation number as predicted by a quantum Pauli master equation (Pauli ME, PME) with average rate of relaxation $\bar{w} = \bar{w}_{qu} = \bar{w}_{cl} = \hat{\gamma}(\omega_0)/2$ (cf. eq 18). Obviously, the latter decay curve falls systematically below the numerical data for the mean occupied state $\langle m \rangle_t$. The same is also true for the decay curve predicted by a quantum/classical PME (eq 23) with $\bar{w} = \bar{w}_{qc} < \bar{w}_{cl}$. Interestingly, the best agreement with the numerical data for $\langle m \rangle_t$ is observed, when a quasi-classical PME is used, where $\bar{w} = \bar{w}_{cl} = 0.2\ ps^{-1}$ (see the model parametrization in section 3.1) and the mean thermal occupation number set equal to its value in the classical limit, $\bar{n}(\omega_0) = \bar{n}_{cl}(\omega_0) = (\beta\hbar\omega_0)^{-1}$. To aid the reader in judging the statistical significance of this result, a numerical data point is included with an error bar indicating the overall statistical uncertainty (<10%).

The results reported and analyzed sofar for the original TFS−SH scheme indicate, that fewest switches surface hopping applied to the case of a damped oscillator apparently fails to reproduce a quantum statistical asymptotic thermal equilibrium for the quantum subsystem, in contrast to the recent suggestion by Parandekar and Tully[41] based on the analysis of a two-level quantum subsystem. Detailed arguments relating our findings to those of Parandekar and Tully will be given later, when discussing our numerical evidence on the issue of quantum thermal equilibrium. While it would be inappropriate to claim that our results obtained for the damped oscillator case represent a generic property of the TFS−SH method, the prediction of a quantum statistical thermal equilibrium can in our view be definitely ruled out for the model situation considered here. Although the length of our current simulations is not sufficient to arrive at a completely thermalized state of the quantum subsystem, it would appear strange to expect the numerical decay curve for $\langle m \rangle_t$ deviating strongly from the prediction of the quasi-classical Pauli ME at later times, when it so accurately followed it up to three times the parametrized energy relaxation time ($\tau_{cl} = \bar{w}_{cl}^{-1} = 5$ ps). The only way of arriving at an asymptotic quantum statistical thermal equilibrium would require the assumption of a nonexponential decay of the average energy (occupation number), including relaxation time(s) much larger than τ_{cl}, a rather unphysical assumption for a linearly damped harmonic oscillator.

Qualitatively, the energy relaxation behavior of the damped oscillator, subject to Tully's TFS−SH scheme, may be rationalized as follows: The quantum amplitudes, and thus the adiabatic populations and coherences, along a single quantum/classical trajectory evolve fully coherently from the quantum initial state, and the influence of the classical environmental forces tends to drive the quantum "reference" state $|\Psi_S(t)\rangle$ to a higher mean energy $\hbar\omega_0\langle \hat{n}_{ad} \rangle_t$ (cf. Figures 2a and 3a). As discussed above, this implies that the "reference" state, i.e., the adiabatic populations and coherences, from which the transition probabilities are determined according to eqs 6 and 7, unduely favors transitions to higher adiabatic energy levels, even though the quantum/classical energy conservation (eq 10) provides an overall "thermodynamic cutoff" for the latter type of transitions, such that transitions to lower energy states win on average. The question, why this should specifically lead to a quasi-classical thermal equilibrium for $\langle m \rangle$, must be left open at this point. However, the ensemble averaged energy relaxation toward $\hbar\omega_0\bar{n}_{cl} = k_BT > \hbar\omega_0\bar{n}(\omega_0, T)$ with the decay time τ_{cl} is qualitatively consistent with the above arguments.

Obviously, something is going wrong with Tully's original fewest switches scheme when applied to the simple problem of a damped quantum oscillator in a classical heat bath. The ensemble averaged mean energy $\hbar\omega_0\langle m \rangle_t$ above the zero point level tends to come out too large, as compared to the expected relaxation toward a quantum statistical equilibrium, and the origins of this behavior can be identified already at the single-trajectory level. As implicitly evident from Figures 2a and 3a, a large discrepancy is observed between the adiabatic energy level populations obtained from the quantum amplitudes and the ones obtained from the occupied state assignment. Yet the adiabatic level populations and coherences derived from the coherently evolving quantum amplitudes are used to obtain the hopping probabilities for the stochastic evolution of the occupied adiabatic state $m(t)$.

While it is true that the evolution of coherences and populations should reflect non-Markovian effects to some extent, which the TFS−SH coherences undoubtedly do, it is also true that the dissipative subsystem should approach a Markovian limit at longer times. In the absence of so-called "pure dephasing", according to Redfield theory (eqs 15, 16, and 19), the phase coherence between energy states on average vanishes on the time scale of local population relaxation. On the single-trajectory level dephasing may either be introduced as a continuous process[25] (using the density matrix) or as a discontinuous, stochastic process (as adopted here). The simplest way of implementing the above connection between dephasing and local population relaxation on the single-trajectory level is to discard the adiabatic coherences after each successful hop, by resetting the state vector to the new assigned adiabatic state. The resultant "collapse" of the coherently evolving quantum state vector onto the new occupied state seems to imply an effective measurement-like interaction between the quantum subsystem and its (classical) surroundings (i.e., quantum decoherence). Objections against this view may, from a more microscopic perspective, be answered as follows: The original TFS−TSH method includes non-Markovian effects in the evolution of the quantum subsystem due to the fact that the

quantum state vector is propagated coherently throughout along each single quantum/classical trajectory. However, after some time interval (defined essentially by the correlation time of the classical force $F(t)$, $\tau_c \sim 100$ *fs* in the present case) the evolution of the quantum distribution $\{p_m(t)\}$ should become independent of its history. This, in turn, implies that the transition rates $w_{m\to n}$ only depend on m and n (and the spectral density of bath forces). In order for this to be true, the ensemble averaged rates in the Markovian limit have to be expressed as $w_{m\to n} = \langle p_{m\to n}(t;\delta t)\rangle_m/\delta t$, where the subscript m now denotes not only constraining the classical dynamics to the m th adiabatic potential energy surface. It also means that the single-trajectory adiabatic populations and coherences, determining the hopping probabilities of eq 7 and thereby the average hopping rates, effectively evolve from a situation where $\rho_{mm}(t_{\text{hop}}) = a_m(t_{\text{hop}})a_m^*(t_{\text{hop}}) \approx 1$, i.e., the rate of escape from state m to state n in the Markovian limit is the same as if m was the initially prepared adiabatic state m_0. This approach to the Markovian limit should be reflected somehow in the single-trajectory implementation of TFS−SH, be it smooth in time or sudden. On a sufficiently coarse-grained time scale, the smooth transition to the Markovian limit may be replaced by a sudden jump to the respective new adiabatic state on the single-trajectory level; i.e., we arrive at the "collapse" or "hopping with complete dephasing" implementation of TFS−TSH as suggested above, which is, however, physically distinct from quantum decoherence (see our later discussion). What follows is an investigation of this modified TFS−SH scheme.

In Figure 2b, for our TFS−TSH with dephasing, the evolution of the assigned occupied adiabatic state $m = \langle m|\hat{n}_{\text{ad}}|m\rangle$ along a single TSH trajectory is shown and compared to the mean adiabatic occupation number $\langle\hat{n}_{\text{ad}}\rangle = \langle\Psi_S(t)|\hat{n}_{\text{ad}}|\Psi_S(t)\rangle$. As is clearly visible, during coherent evolution between quantum transitions the classical heat bath tends to drive the quantum subsystem to a higher mean energy ($\langle\hat{n}_{\text{ad}}\rangle$), again a behavior which is similar to mean field Ehrenfest dynamics starting from an (excited) energy eigenstate.[33,34] The discrepancy between m and $\langle\hat{n}_{\text{ad}}\rangle$ becomes particularly pronounced when $m = 0$, where only the thermally activated channel $0\to1$ is possible, and enough kinetic energy must be available along the nonadiabatic coupling vector $\mathbf{d}_{01}$, in order for the hop to occur. The coherent time interval (waiting time) in $m = 0$ is therefore comparatively long. Although $\langle\hat{n}_{\text{ad}}\rangle \geq m$, the evolution of $\langle\hat{n}_{\text{ad}}\rangle$ closely follows the assigned adiabatic state index m (the "occupied" state), due to our procedure of resetting the wave packet to the new adiabatic state (and the adiabatic coherences to zero) immediately after a transition $m\to n$, such that the coherent cycle then starts again with $\langle\hat{n}_{\text{ad}}\rangle = n$ and $p_n = 1$. However, by introducing dephasing in the adiabatic basis, as implemented here, coherence effects are not maintained across transitions between adiabatic states. Rather, it is ensured that the transition rates $w_{m\to n}$ originating from state m are always the same, independent of the initialization (m_0) and the history of the evolving ensemble $\{p_m(t)\}$.

Figure 3b, for our modified TFS−SH scheme, shows the ensemble averaged data for $\langle m\rangle$ and $\langle\hat{n}_{\text{ad}}\rangle$. Again, $\langle\hat{n}_{\text{ad}}\rangle \geq \langle m\rangle$ as in the single-trajectory case. The deviation becomes particularly large at low energies close to thermal equilibrium, for reasons that have been discussed above. Also shown is the decay of mean occupation number as predicted by a quantum/classical PME, eqs 21−23, with $\bar{w} = \bar{w}_{qc} \leq \bar{w}_{cl}$. In the present case, $\bar{w}_{cl} = 0.2\ \text{ps}^{-1}$ and $\bar{w}_{qc} \cong 0.895 \times 0.2\ \text{ps}^{-1}$. The agreement of the Q/C PME with $\langle m\rangle$ already demonstrates, that fewest switches TSH (including dephasing) applied to a harmonic oscillator with linear dissipation (i) gives a quantum statistical asymptotic thermal equilibrium for the quantum subsystem, and (ii) is equivalent to a (particular) quantum/classical PME treatment as traditionally employed in the field of vibrational energy relaxation.[55,56] It also underscores, that quantum statistical dynamical information should always be derived from the statistics of assigned adiabatic states m.[11] Comparison of numerical results to the quantum PME prediction ($\bar{w} = \bar{w}_{qu} = \bar{w}_{cl}$), on the other hand, shows that the latter decay curve falls systematically below the numerical one. Again, a numerical data point is included with an error bar indicating the overall statistical uncertainty (<10%) and pointing out the statistical significance of our findings.

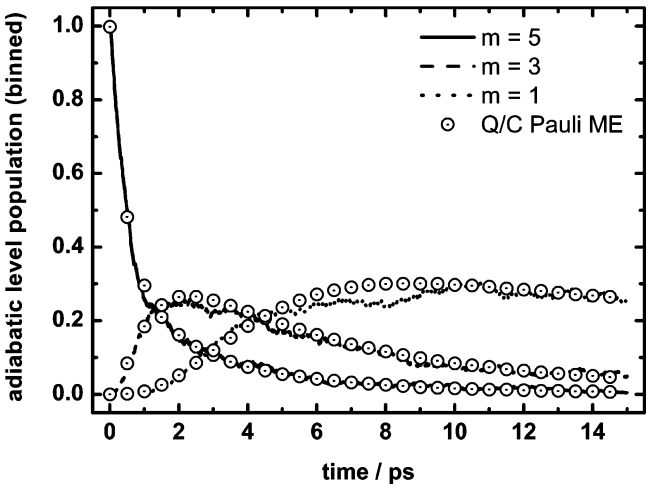

Figure 4. Ensemble averaged time evolution of adiabatic energy level populations for quantum numbers $m = 5$ (initially occupied), 3, and 1, compared to the quantum/classical PME prediction (modified TFS−SH).

Figure 3c contains, in addition to the first moment $\langle m\rangle$, also the standard deviation $\sigma_m = \sqrt{\langle m^2\rangle - \langle m\rangle^2}$. Again, the agreement with the quantum/classical PME is satisfactory.

Besides the analysis given sofar, we observe that the relaxation of $\langle\hat{n}_{\text{ad}}\rangle$ very accurately follows the exponential decay law of eq 23 with $\bar{w} = \bar{w}_{cl}$ and $\bar{n} = \bar{n}_{cl} = (\beta\hbar\omega_0)^{-1}$, i.e., relaxation toward a quasi-classical thermal equilibrium, the same type of relaxation behavior exhibited by the mean occupied state $\langle m\rangle$ for Tully's original TFS−TSH (Figure 3a). This is not shown here but reserved for further consideration.

In the following, we refer to our modified version of Tully's fewest switches method, except when indicated otherwise.

3.2.2. Population Relaxation. A more detailed view is provided by the population dynamics (Figure 4) as derived from the statistics of assigned adiabatic states ("binned" populations). Along a single TFS−TSH trajectory, probabilities are assigned as $p_m(t) = 1$ (occupied state) and $p_n(t) = 0$ ($n \neq m$), respectively. Figure 4 contains the ensemble averaged data for $m = 5$, 3, and 1 as compared to the quantum/classical PME prediction. Especially the decay of higher excited states ($m = 5$ and 3) is very well reproduced, while for the first excited state, which is significantly populated at thermal equilibrium, it is more difficult to average out thermal fluctuations. Thus, we have strong arguments for the equivalence between both types of quantum/classical approaches, at least within the limits of numerical accuracy and finite ensemble size. This equivalence is, in our view, by no means a priori self-evident and will be addressed below by statistical theory based on the TFS−SH scheme.

Furthermore, the approach to quantum statistical equilibrium of the quantum subsystem is numerically demonstrated by

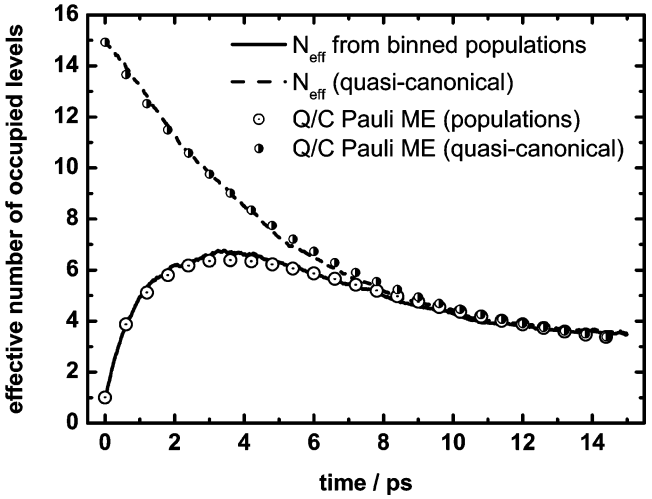

Figure 5. Time evolution of the nonequilibrium entropy $S(t) = \ln N(t)$ (in terms of an effective number of occupied energy levels) as calculated from the adiabatic energy level populations and as obtained from the mean occupied adiabatic state (assuming a quasi-canonical distribution), compared to the quantum/classical PME prediction (modified TFS−SH).

exploiting the property that the populations of harmonic oscillator eigenstates at thermal equilibrium

$$p_n = \left(\frac{\bar{n}}{\bar{n}+1}\right)^n \frac{1}{\bar{n}+1} \tag{28}$$

are solely determined by the mean thermal occupation number $\bar{n}(\omega_0, T)$.[59] The nonequilibrium distribution $\{p_n(t)\}$ may be globally characterized via the information entropy[59,60]

$$S(t) = -\sum_m p_m(t) \ln p_m(t) = \ln N_{\text{eff}}(t)$$

$$S_{\text{canonical}}(t) = (\langle m\rangle_t + 1)\ln(\langle m\rangle_t + 1) - \langle m\rangle_t \ln\langle m\rangle_t \tag{29}$$

where $S_{\text{canonical}}(t)$ corresponds to a (nonequilibrium) canonical distribution, to which a temperature may be assigned, and $N_{\text{eff}}(t)$ is an effective number of uniformly occupied energy levels.[34] Figure 5 shows that $S(t)$ ($N_{\text{eff}}(t)$), derived from binned adiabatic populations, converges to $S_{\text{canonical}}(t)$ ($N_{\text{canonical}}(t)$), as derived from the mean occupied state $\langle m\rangle_t$, and both are in very satisfactory agreement with the quantum/classical Pauli master equation. Although at $t = 15$ ps the adiabatic populations have not yet relaxed to $T = T_{\text{bath}}$ (300 K), the distribution has reached a quasi-thermal form ($T > T_{\text{bath}}$). It is well-known and easy to show that a quasi-canonical distribution analoguous to eq 28, with $\bar{n}(\omega_0, T)$ replaced by $\langle\hat{n}\rangle_t$, is stable in its analytical form subject to a Pauli master equation with the detailed-balanced rate coefficients given by eqs 18 or 22, such that only the mean occupation number $\langle\hat{n}\rangle_t$ changes according to the linear rate law, eq 23. Thus, the fact, that the populations of adiabatic energy levels have arrived at a (still nonequilibrium) quasi-canonical form well before $t = 15$ ps, reflecting the detailed balance property of our numerical TFS−TSH rate coefficients $\langle p_{m\to n}(t;\delta t)\rangle/\delta t$, provides in our view strong support for the argument that the distribution will continue in following the evolution toward a quantum statistical thermal equilibrium as predicted by the quantum/classical PME.

3.2.3. Statistical Theory: TFS—TSH Quantum/Classical Master Equation. In the following, statistical theory is applied in an attempt to derive the hopping rates $w_{m\to n}$ of the Pauli master equation, eq 11, from the TFS−SH scheme (with dephasing), eqs 2, 6, 7, 10, and 24, and the underlying model Hamiltonian, eq 12. For the harmonic oscillator with linear damping, the vibrationally adiabatic states are again (displaced) HO eigenfunctions, centered at the origin

$$q_0[\mathbf{Q}(t)] = \frac{F(t)}{\mu\omega_0^2} \to \hat{q} = \delta\hat{q}[\mathbf{Q}(t)] + q_0[\mathbf{Q}(t)] \tag{30}$$

with displacement $\delta\hat{q}(t)$ and $F(t) = \sum_l g_l Q_l(t)$. The adiabatic states $|\chi_m[\mathbf{Q}(t)]\rangle$ are eigenstates of $\hat{H}_q[q;\mathbf{Q}(t)]$, eqs 2 and 24, which may be rewritten as

$$\begin{aligned}\hat{H}_q[q;\mathbf{Q}(t)] &= \frac{\hat{p}^2}{2\mu} + \frac{\mu\omega_0^2}{2}\hat{q}^2 - \hat{q}\,F(t)\\ &= \frac{\hat{p}^2}{2\mu} + \frac{\mu\omega_0^2}{2}(\delta\hat{q}(t))^2 - \frac{\mu\omega_0^2}{2}(q_0(t))^2\\ &= \hbar\omega_0\left(\hat{n}_{\text{ad}}[\mathbf{Q}(t)] + \frac{1}{2}\right) - \frac{\mu\omega_0^2}{2}(q_0(t))^2\end{aligned} \tag{31}$$

And the eigenvalues are

$$\epsilon_m[\mathbf{Q}(t)] = \hbar\omega_0\left\{m + \frac{1}{2}\right\} - \frac{\mu\omega_0^2}{2}(q_0(t))^2 \tag{32}$$

The matrix elements $q_{mn}[\mathbf{Q}(t)]$ in the adiabatic basis are easily evaluated to

$$q_{mn}[\mathbf{Q}(t)] = q_0[\mathbf{Q}(t)]\delta_{mn} + \sqrt{\frac{\hbar}{2\mu\omega_0}}\{\sqrt{n}\,\delta_{m,n-1} + \sqrt{n+1}\,\delta_{m,n+1}\} \tag{33}$$

and determine the classical equations of motion, eq 24, via

$$\dot{P}_l(t) = -\omega_l^2 Q_l(t) + g_l q_0[\mathbf{Q}(t)] \tag{34}$$

as well as the nonadiabatic coupling vector, with components (eq 4)

$$d^{(l)}_{mn}[\mathbf{Q}(t)] = +\frac{g_l\, q_{mn}[\mathbf{Q}(t)]}{\hbar\omega_0(m-n)} = -d^{(l)}_{nm}[\mathbf{Q}(t)] \tag{35}$$

which are time-independent in the present case (eq 33, $m \neq n$). The nonadiabatic coupling is, therefore, simply given by

$$\mathbf{d}_{mn}[\mathbf{Q}(t)]\cdot\dot{\mathbf{Q}}(t) = \frac{q_{mn}}{\hbar\omega_{mn}}\dot{F}(t), \qquad \dot{F}(t) = \sum_l g_l P_l(t) \tag{36}$$

Equations 33, 35, and 36 imply that the vibrationally nonadiabatic coupling is delocalized in the phase space (position space) of the classical environmental degrees of freedom.

The adiabatic coherences evolving from $\rho_{mm}(t) = \rho_{mm}[t;\mathbf{Q}(t)] = 1$ ($t \to 0$) at short times are

$$\rho_{mn}(t) \simeq -\int_0^t \mathrm{d}t'\, \mathrm{e}^{-i\omega_{mn}(t-t')}\, \mathbf{d}_{mn}\cdot\dot{\mathbf{Q}}(t')\{\rho_{nn}(t') - \rho_{mm}(t')\} \tag{37}$$

where $t = t_{\text{hop}} = 0$ is understood as the time origin of a coherent propagation cycle. Immediately after a surface hop ($t \geq t_{\text{hop}}$), due to our "hopping with complete dephasing" ansatz, we have

$\rho_{nn}(t) \simeq \delta_{mn}$, where m is the occupied state. Insertion into eq 5 yields the (single-trajectory) rate equation (cf. eqs 6 and 7)

$$\frac{\mathrm{d}}{\mathrm{d}t}\rho_{mm}(t) = -\sum_{n\neq m}\frac{t_{m\to n}(t;\delta t)}{\delta t} \simeq -\sum_{n\neq m}\{\kappa_{m\to n}(t)\,\rho_{mm}(t) - \kappa_{n\to m}(t)\,\rho_{nn}(t)\}$$

$$\kappa_{m\to n}(t) = \frac{|q_{mn}|^2}{(\hbar\omega_{mn})^2}\int_0^t \mathrm{d}t'\,\{\mathrm{e}^{-i\omega_{nm}(t-t')} + \mathrm{e}^{+i\omega_{nm}(t-t')}\}\dot{F}(t)\dot{F}(t') \tag{38}$$

to second order in the nonadiabatic coupling (system−bath interaction), in the Markovian approximation, $\rho_{mm}(t') \simeq \rho_{mm}(t)$. The apparent symmetry in the single-trajectory rate coefficients, $\kappa_{n\to m}(t) = \kappa_{m\to n}(t)$ (eq 38), is broken by the requirement of quantum/classical energy conservation, $K_n + \epsilon_n[\mathbf{Q}(t)] = K_m + \epsilon_m[\mathbf{Q}(t)]$, during hopping (see below). Ensemble averaging over the classical heat bath variables thus gives the rate coefficients

$$w_{m\to n}(t) = \left\langle\frac{t_{m\to n}(t;\delta t)}{\delta t\,\rho_{mm}(t)}\right\rangle \simeq \langle\kappa_{m\to n}(t)\rangle = \frac{|q_{mn}|^2}{(\hbar\omega_{mn})^2}\int_0^t \mathrm{d}t'\{\mathrm{e}^{-i\omega_{nm}(t-t')} + \mathrm{e}^{+i\omega_{nm}(t-t')}\}\langle\dot{F}(t)\dot{F}(t')\rangle_{m\to n} \tag{39}$$

of a quantum/classical Pauli master equation (eq 11), where the subscript $m\to n$ indicates sampling in the adiabatic state m and observing the energy conservation constraint for $m\to n$. If $\dot{F}(t)$ can be considered a stationary random process, $\langle\dot{F}(t)\dot{F}(t')\rangle \cong \langle\dot{F}(t-t')\dot{F}(0)\rangle$, the transition rates ($t\to\infty$) may be written in the Golden Rule form

$$w_{m\to n} = \frac{|q_{mn}|^2}{(\hbar\omega_{mn})^2}\int_{-\infty}^{+\infty}\mathrm{d}\tau\,\mathrm{e}^{-i\omega_{nm}\tau}\,\langle\dot{F}(\tau)\dot{F}(0)\rangle_{m\to n} = \frac{|q_{mn}|^2}{\hbar^2}\int_{-\infty}^{+\infty}\mathrm{d}\tau\,\mathrm{e}^{-i\omega_{nm}\tau}\langle F(\tau)F(0)\rangle_{m\to n} \tag{40}$$

using $\langle\dot{F}(\tau)\dot{F}(0)\rangle = -\langle\ddot{F}(\tau)F(0)\rangle$. Note, however, that the bath oscillators are coupled to each other (eq 34) through $q_0(t)$ (eq 30). The implications are discussed below.

In fewest switches TSH, the bath force (time-derivative) correlation function is implicitly sampled subject to the constraint (cf. eq 10)

$$(\mathbf{P}_m\cdot\mathbf{e}_{mn})^2 = \frac{(\dot{F}(t))^2}{\sum_l g_l^2} \geq 2\hbar\omega_{nm} = 2\hbar\omega_0(n-m) \tag{41}$$

where $\mathbf{e}_{mn} = \mathbf{d}_{mn}/\sqrt{\mathbf{d}_{mn}\cdot\mathbf{d}_{mn}} = \mathbf{g}/\sqrt{\sum_l g_l^2}$. The bath correlation function appearing in eq 39 may then be expressed as

$$\langle\dot{F}(t)\dot{F}(t')\rangle_{m\to n} = \int d\mathbf{P}d\mathbf{Q}\;\rho(\mathbf{Q},\mathbf{P};t)\,\dot{F}(t)\dot{F}(t')\Theta[x(t)] \simeq \int d\mathbf{P}d\mathbf{Q}\;\rho_{\mathrm{eq}}(\mathbf{Q},\mathbf{P})\,\dot{F}(0)\dot{F}(-\tau)\Theta[x(0)] \tag{42}$$

where $\Theta[x(t)] = \Theta[(\dot{F}(t))^2 - 2\hbar\omega_{nm}\sum_l g_l^2]$ is the step function, $\tau = t - t'$, and the second line follows from the assumption $\rho(\mathbf{Q},\mathbf{P};t) \simeq \rho(\mathbf{Q},\mathbf{P};0) = \rho_{\mathrm{eq}}(\mathbf{Q},\mathbf{P})$. The latter corresponds to the standard assumption made in situations where a small system is coupled to a large but finite heat reservoir: Although the relevant subsystem perturbs the environment causing it to deviate from its initial equilibrium, this deviation may be assumed irrelevant as long as the heat bath is large enough. In the present case of a nonergodic reservoir this assumption may still be used, because the exchange of energy quanta $\hbar\omega_{nm}$ is distributed over a large number of bath DoF, according to the prescription for the momentum adjustment in TFS−SH (eqs 9 and 10) and the nature of system−bath interaction (eqs 35 and 36).

Before evaluating eq 42, we need to consider the properties of $\dot{F}(t)$. First, the force $F(t) = \sum_l g_l Q_l(t)$ is obtained by integrating the classical equations of motion (eq 34) to[48]

$$F(t) = F_{\mathrm{B}}(t) - \int_0^t \mathrm{d}s\;\mu\dot{\gamma}(t-s)\,q_0(s)$$

$$F_{\mathrm{B}}(t) = \sum_l g_l\left\{Q_l(0)\cos\omega_l t + \frac{P_l(0)}{\omega_l}\sin\omega_l t\right\} \tag{43}$$

where $F_B(t)$ is a random force originating from the free bath initial conditions, and $\gamma(t)$ is the friction kernel of the GLE, eqs 13 and 14. The force time-derivative $\dot{F}(t)$, as obtained from eq 43 and partial integration, is

$$\dot{F}(t) = \dot{F}_{\mathrm{B}}(t) - \int_0^t \mathrm{d}s\;\mu\ddot{\gamma}(t-s)\,q_0(s) = \delta\dot{F}(t) - \int_0^t \mathrm{d}s\;\mu\dot{\gamma}(t-s)\,\dot{q}_0(s)$$

$$\delta F(t) = \sum_l g_l\left\{\left(Q_l(0) - \frac{g_l}{\omega_l^2}q_0(0)\right)\cos\omega_l t + \frac{P_l(0)}{\omega_l}\sin\omega_l t\right\} = F_{\mathrm{B}}(t) - \mu\gamma(t)q_0(0) \tag{44}$$

using $\dot{\gamma}(t=0) = 0$. $\delta F(t)$ is now a random force with shifted bath initial conditions,[48,52] analoguous to the one appearing in the GLE, eq 13. Its statistical properties are given by eq 14. More specifically, this applies only in the absence of the TFS−TSH energy conservation restrictions as expressed by eqs 41 and 42 ($n < m$). The force time-derivative of eq 44 is nonstationary in general, it is coupled to its own history through $\dot{q}_0(s) = \dot{F}(s)/\mu\omega_0^2$. Note, however, that $\lim_{t\to 0}\dot{F}(t) = \delta\dot{F}(t)$.

Since the memory in the time-evolution of $\dot{F}(t)$ is related to (the time-derivative of) the friction kernel, which in turn expresses the weak time-retarded frictional coupling of the quantum subsystem to its (classical) environment, it may be assumed that the dominant contribution to $\dot{F}(t)$ is $\delta\dot{F}(t)$. The influence of the bilinear coupling between bath oscillators (cf. eq 34) may be taken into account perturbatively. To second order, we have

$$\dot{F}(t) = \delta\dot{F}(t) - \frac{1}{\omega_0^2}\int_0^t \mathrm{d}s\;\dot{\gamma}(t-s)\,\delta\dot{F}(s) \tag{45}$$

Here, we restrict ourselfs to zeroth order, $\dot{F}(t) \simeq \delta\dot{F}(t)$, and argue that the coupling between oscillators mainly serves to maintain thermal equilibrium between the bath DoF.

Equation 42 is difficult to evaluate analytically in general, except for downward transitions ($n < m$), where $\langle\dot{F}(t)\dot{F}(t')\rangle \simeq \langle\delta\dot{F}(t)\delta\dot{F}(t')\rangle = -\mu k_B T\ddot{\gamma}(t-t')$. In particular, it is not at all evident that the step function $\Theta[(\dot{F}(t))^2 - 2\hbar\omega_{nm}\sum_l g_l^2]$, intro-

duced in eq 42 to account for quantum/classical energy conservation (eqs 10 and 41), should generally yield the quantum detailed balance property $w_{m\to n}/w_{n\to m} = e^{-\beta\hbar\omega_{nm}}$ for the transition rates $w_{m\to n}$ of eq 40. Here, we simply bypass this problem and *assume* that the energy conservation constraint introduces (roughly) a factor of $e^{-\beta\hbar\omega_{nm}}$ for $n > m$ (upward transitions), and unity for $n < m$. The (approximate) validity of quantum detailed balance has been demonstrated numerically above (see also the analysis below, based on the fraction of rejected hops). Because of the ad hoc inclusion of quantum/classical energy conservation, the equilibrium density $\rho_{eq}(\mathbf{Q},\mathbf{P})$ in eq 42, and thus the force correlation spectrum (eq 40), should be rescaled by the average fraction, $(1 + e^{-\beta\hbar\omega_0})/2$ for the damped HO, of successful escape events from state m into states $n = m \pm 1$. Thus, for the linearly damped harmonic oscillator we obtain the transition rates

$$w_{m\to m+1} = \frac{m+1}{2\mu\hbar\omega_0}\hat{C}_{cl}(\omega_0)\frac{2e^{-\beta\hbar\omega_0}}{1+e^{-\beta\hbar\omega_0}} = \frac{2k_BT}{\hbar\omega_0(2\bar{n}+1)}\frac{\hat{\gamma}(\omega_0)}{2}\bar{n}(m+1)$$

$$w_{m\to m-1} = \frac{m}{2\mu\hbar\omega_0}\hat{C}_{cl}(\omega_0)\frac{2}{1+e^{-\beta\hbar\omega_0}} = \frac{2k_BT}{\hbar\omega_0(2\bar{n}+1)}\frac{\hat{\gamma}(\omega_0)}{2}(\bar{n}+1)m \quad (46)$$

which coincide with the quantum/classical transition rates reported in eq 22, and we recover Oxtoby's quantum prefactor[55] from the TFS−TSH scheme (eqs 2−10 and 24) and, importantly, our dephasing procedure (implicit in eqs 37−40). This is a remarkable result. Although we have obtained it via a rather bold heuristic assumption regarding the issue of detailed balance, this result is expected to hold (for the damped harmonic oscillator) whenever the system−bath interaction potential is dominated by the linear term $-\hat{q}F(t)$, where the bath force $F(t)$ may be an arbitrary function of the positions of environmental DoF, in other words, whenever the phenomenological applicability of a generalized Langevin equation (eq 13) may be assumed. In particular, if the above rate theory applies to situations with a large but *nonergodic* heat bath, it appears natural to assume its validity also (and all the more) for *ergodic* heat reservoirs, as long as multiphonon effects of bath degrees of freedom[56,61] (especially relevant for high-frequency solute oscillators) are not important. Note, however, that the transition rates of eq 46 correspond to a special case only of the more general rate expression eq 21, obtained as a quantum/classical approximation to the quantum rate formula eq 16 via Oxtoby's correspondence $\hat{C}_+(\omega) \simeq \hat{C}_{cl}(\omega)$ and quantum detailed balance (eqs 17 and 20). Whether the more general quantum/classical rate expression of eq 21 is also reproduced by TFS−SH (with dephasing) for a linearly damped *anharmonic* oscillator, where the vibrationally adiabatic states cannot be obtained analytically, can only be decided by numerical simulation.

Before we provide additional numerical evidence for quantum detailed balance being (approximately) obeyed by our modified surface hopping scheme, we discuss in more detail various origins of dephasing/decoherence as related to the validity of our quantum/classical rate expression, eq 40.

3.2.4. Pure Dephasing and Energy Relaxation vs Quantum Decoherence. Up to now, we have discussed the issue of dephasing mainly from the perspective of a Redfield master equation (eq 15) in the secular limit. In particular, in the absence of pure dephasing the process of population relaxation (energy relaxation) gives rise to a loss of phase coherence between energy levels (eq 19). Here we discuss dephasing/decoherence in the context of quantum/classical dynamics from a broader perspective, using more precise terminology, by focusing on the poineering approach of Rossky and coworkers.[29,30,31,62]

As noted by Rossky,[31] the origins of dephasing (in quantum/classical dynamics) basically include two components. The first is due to fluctuations of the energy levels involved in transitions, i.e., due to the effect of a classical-like random external field coupled "diagonally" to the energy states of the quantum subsystem. This component naturally appears as pure dephasing in a quantum/classical setting, as a result of the adiabatic energy states $\epsilon_m[\mathbf{Q}(t)]$ being parametrically dependent on the classical coordinates. Averaging over classical initial conditions then leads to a fading out of the statistically superposed individual phase factors $e^{-i\int_0^t d\tau\omega_{nm}[\mathbf{Q}(\tau)]}$ as, for example, in Kubo's stochastic theory of line shape via random frequency modulation.[60] In the present context, this requires that the adiabatic energy levels $\epsilon_m[\mathbf{Q}(t)] = \hbar\omega_m[\mathbf{Q}(t)]$ are shifted differently, and therefore relative to one another, by the motion of classical external degrees of freedom. The phase factors $e^{-i\int_0^t d\tau\omega_{nm}[\mathbf{Q}(\tau)]}$, primarily reflecting the evolution of coherences, indirectly affect the quantum/classical transition rates $w_{m\to n}$ (cf. eqs 37−40). Note that dephasing related to energy dissipation/population relaxation (lifetime broadening of energy levels), as introduced in this paper, may intuitively also be grouped into this category. It is, however, physically distinct from pure dephasing, since it originates from a "nondiagonal" coupling (to the environment), causing the subsystem to change state. In a quantum trajectory picture, these state changes (transitions) occur at random times distributed according to the microscopic transition rates, thereby interrupting the coherent evolution of the subsystem and leading to dephasing of an ensemble of subsystems. In contrast to pure dephasing, dephasing due to population relaxation is not naturally included in single-trajectory quantum/classical dynamics methods and must be introduced in an ad hoc manner (if considered important). As will become apparent below, the quantum/classical pure dephasing effects, although being an ensemble phenomenon, seem to have much in common with quantum decoherence, to be discussed below, since both effects crucially depend on the difference of "forces" exerted on the environment by different states of the subsystem. This statement is, however, to be understood with some caution,[26,27] due to our lack of classical analogues for quantum decoherence.

The second component of dephasing, as noted by Rossky, is of a genuinely quantum mechanical origin and is referred to as quantum decoherence in the more narrow sense of the meaning.[26−28] It emerges as follows: Consider for simplicity a two-state quantum subsystem $\mathcal{S}$ with basis states $|0\rangle$ and $|1\rangle$, initially in a superposition state $|\Psi_{\mathcal{S}}\rangle = a_0|0\rangle + a_1|1\rangle$, which interacts with an environment $\mathcal{E}$, initially in some state $|i_{\mathcal{E}}\rangle$. So the total system $\mathcal{SE}$ is considered initially in a pure, uncorrelated state (product state) $|\Psi\rangle = |\Psi_{\mathcal{S}}\rangle|i_{\mathcal{E}}\rangle$, where the possibility of initial entanglement is neglected here. As the total system evolves under the action of the Hamiltonian, its initial state will generally be turned into an entangled state, i.e., a superposition of product states

$$|\Psi\rangle = (a_0|0\rangle + a_1|1\rangle)|i_E\rangle \xrightarrow{e^{-iHt/\hbar}} |a_0^{(\mathcal{E})}(t)\rangle|0\rangle + |a_1^{(\mathcal{E})}(t)\rangle|1\rangle \quad (47)$$

where the conditional state vectors $|a_m^{(\mathcal{E})}(t)\rangle$ correspond to close-coupling amplitudes (partial wave packets) of the environment, with their norms $\langle a_m^{(\mathcal{E})}(t)|\ a_m^{(\mathcal{E})}(t)\rangle = p_m(t)$ equal to the probability of occurrence of the subsystem state $|m\rangle$. The states $|0\rangle$ and $|1\rangle$ may be the Born−Oppenheimer ground and (first) excited states of a large molecule or electronic impurity states in a liquid or solid, and $|a_m^{(\mathcal{E})}(t)\rangle$ ($m = 0, 1$) the partial nuclear wave packets associated with the (adiabatic or diabatic) electronic states involved. The overlaps $J_{mn}(t) = \langle a_m^{(\mathcal{E})}(t)|a_n^{(\mathcal{E})}(t)\rangle$ for $m \neq n$ need not equal zero. To the extent, however, that the forces on the environmental degrees of freedom depend on the subsystem state $|m\rangle$, the overlaps $J_{mn}(t)$ will more or less quickly decay to zero. The subsystem reduced density matrix (in the $\{|m\rangle\}$-basis) is obtained as

$$\hat{\rho}_{\mathcal{S}}(t) = \mathrm{Tr}_{\mathcal{E}}|\Psi(t)\rangle\langle\Psi(t)| = \begin{pmatrix} p_1(t) & J_{01}(t) \\ J_{10}(t) & p_0(t) \end{pmatrix} \tag{48}$$

where $\rho_{mm}(t) = p_m(t) = J_{mm}(t)$ and $\rho_{mn}(t) = J_{nm}(t)$. For a general Hamiltonian $\hat{H} = |0\rangle\hat{H}_{00}^{(\mathcal{E})}\langle 0| + |1\rangle\hat{H}_{11}^{(\mathcal{E})}\langle 1| + \hat{V}$ it is easily seen, that quantum decoherence in the $\{|m\rangle\}$-basis, in order be operative, requires that the environmental Hamiltonian $\hat{H}_{mm}^{(\mathcal{E})}$ is sufficiently dependent on the subsystem state $|m\rangle$, i.e., sufficiently strong "diagonal" system-environment interaction. To zeroth order in the interstate coupling $\hat{V} = |0\rangle\hat{V}_{01}^{(\mathcal{E})}\langle 1| + |1\rangle\hat{V}_{10}^{(\mathcal{E})}\langle 0|$, the evolution of overlaps (cf. eq 47) is obtained as

$$\begin{aligned} J_{mn}^{(0)}(t) &= \langle a_m^{(\mathcal{E};0)}(t)|\ a_n^{(\mathcal{E};0)}(t)\rangle \\ &= a_m^* a_n \left\langle i_{\mathcal{E}}\middle|\exp\left\{\frac{i}{\hbar}\hat{H}_{mm}^{(\mathcal{E})}t\right\}\exp\left\{-\frac{i}{\hbar}\hat{H}_{nn}^{(\mathcal{E})}t\right\}\middle|i_{\mathcal{E}}\right\rangle \end{aligned} \tag{49}$$

Thus, as the overlaps of conditional environmental states $|a_m^{(\mathcal{E})}(t)\rangle$ tend to zero, the subsystem reduced density operator becomes diagonal in the $\{|m\rangle\}$-basis (eq 48). If this occurs rapidly enough, quantum decoherence significantly precedes population relaxation, since $p_m^{(0)}(t) = J_{mm}^{(0)}(t) = |a_m|^2$ to zeroth order in $\hat{V}$. On longer time scales, the balance between the creation of coherences (via the interstate coupling) and their decay (via quantum decoherence) leads to population (energy) relaxation in the subsystem, which in turn defines an upper limit for the time scale of dephasing (eq 19). Note, however, that we have left open the precise nature of the (electronic) states $|0\rangle$ and $|1\rangle$. They may correspond to adiabatic (Born−Oppenheimer) or diabatic molecular energy states, with the interstate coupling term $\hat{V}$ interpreted appropriately. The emergence of the decoherent or pointer basis[26,27] may then intuitively be anticipated as the result of the interplay between the nondiagonal interstate coupling and the diagonal system-environment interaction. In general, at least the initial state of the environment is not a pure state, which introduces the requirement of averaging over different pure state evolutions $|\Psi_{\mathcal{S}}\rangle|\ i_{\mathcal{E}}\rangle \rightarrow |a_0^{(i,\mathcal{E})}(t)\rangle|0\rangle + |a_1^{(i,\mathcal{E})}(t)\rangle|1\rangle$ of the total system, with appropriate statistical weights $w_{i,\mathcal{E}}$. In any case, the underlying mechanism of quantum decoherence, and the associated loss of purity of the subsystem (eqs 48−49), operates at the level of individual pure state evolutions of the total system (eq 47). For quantum/classical pure dephasing, the individual member of the subsystem ensemble does not suffer a loss of purity.

At this point we may already draw some general conclusions on the nature of the decoherent basis in quantum/classical simulations of condensed phase vibrational energy transfer. The quantum/classical system-environment interaction is of some form $\hat{V}[q;\mathbf{Q}(t)]$ (cf. eqs 1 and 2), i.e., diagonal in the space of $\hat{q}$-eigenstates. Specifically, we have chosen the simple form $\hat{V}_{SB} = -\hat{q}\sum_l g_l Q_l(t)$. Quantum decoherence is, therefore, expected to occur effectively in phase space,[27] keeping a balance between localization in position- and momentum-space. If we insist to work in a (diabatic or adiabatic) energy basis $\{|n\rangle\}$, which surface hopping methods obviously imply, the system−bath interaction necessarily involves interstate (nondiagonal) couplings $V_{mn}[q,\mathbf{Q}(t)]$ (or respective kinetic couplings between adiabatic states), and maybe also significant diagonal terms $V_{mm}[q,\mathbf{Q}(t)]$ ($\epsilon_m[\mathbf{Q}(t)]$). Whether quantum decoherence will occur to an appreciable degree in the energy basis chosen, will be determined by the state dependence of the diagonal terms and the relative strength of interstate coupling. In the present model situation, the system-environment interaction is exclusively *nondiagonal*, both in the diabatic (bare solute) vibrational energy basis, $V_{mn}^{(dia)}(t) = -q_{mn}\sum_l g_l Q_l(t)$, and in the vibrationally adiabatic energy basis, $V_{mn}^{(adia)}(t) = -i\hbar\sum_l d_{mn}^{(l)}\dot{Q}_l(t)$ (eqs 32−36). Quantum decoherence is, therefore, predicted to be rigorously absent in both energy bases (see below). We note, however, that the significance of dephasing as related to energy/population relaxation is left untouched by this argument.

Prezhdo and Rossky[31,62] have implemented the above ideas in the domain of quantum/classical surface hopping dynamics starting from the semiclassical frozen Gaussian wave packet (GWP) approach of Neria and Nitzan.[63] Within the limits of second-order perturbation theory, a Golden Rule expression for the quantum rate of a nonadiabatic transition $m \rightarrow n$ may be obtained as[62]

$$w_{m\rightarrow n}^{(qm)} = \frac{1}{\hbar^2}\int_{-\infty}^{+\infty} \mathrm{d}t\ \langle V_{mn}^{(qc)}(t)V_{nm}^{(qc)}(0)\ J^{(mn)}(t)\rangle_{\mathrm{B}} \tag{50}$$

where $V_{mn}^{(qc)}(t) = -i\hbar\mathbf{d}_{mn}[\mathbf{Q}(t)]\cdot\dot{\mathbf{Q}}(t)$ (in our notation) is the quantum/classical nonadiabatic coupling between adiabatic states (eqs 3−5), written as a Hamiltonian term and evolved on the initial adiabatic potential energy surface $\epsilon_m[\mathbf{Q}(t)]$, and the averaging $\langle ...\rangle_{\mathrm{B}}$ is done over a classical initial distribution. The meaning of the overlap $J^{(mn)}(t)$ is somewhat different from above, yet closely related. It is defined as the overlap $J^{(mn)}(t) = \langle G^{(m)}(t)|G^{(n)}(t)\rangle$ of two frozen GWPs[64] evolving on states m and n

$$\begin{aligned} |G^{(m)}(t)\rangle &= \prod\nolimits_l |G_l^{(m)}(t)\rangle\exp\left\{\frac{i}{\hbar}\int_0^t \mathrm{d}\tau\ L_m(\tau)\right\} \\ G_l^{(m)}(Q_l, P_l;t) &= \sqrt[4]{\frac{a_l}{\pi}}\exp\left\{-\frac{a_l}{2}[Q_l - Q_l^{(m)}(t)]^2 + \right. \\ &\qquad \left. \frac{i}{\hbar}P_l^{(m)}(t)[Q_l - Q_l^{(m)}(t)]\right\} \end{aligned} \tag{51}$$

composed of a product of single-particle (single-DoF) Gaussians $|G_l^{(m)}(t)\rangle$, which are characterized by position and momentum parameters $Q_l^{(m)}(t)$ and $P_l^{(m)}(t)$, respectively, governed by classical dynamics on the m th potential energy surface, and a fixed real valued width parameter a_l. The overall phase factor contains the classical Lagrangian $L_m(t) = K(t) - \epsilon_m[\mathbf{Q}(t)]$. Consequently,

the complex valued overlap $J^{(mn)}(t)$ may be written as a product of nuclear overlap and phase terms[62−64]

$$J^{(mn)}(t) = J^{(mn)}_{\text{overlap}}(t)\, J^{(mn)}_{\text{phase}}(t)$$

$$J^{(mn)}_{\text{overlap}}(t) = \prod_l \langle G^{(m)}_l | G^{(n)}_l(t)\rangle$$

$$= \prod_l \exp\left\{ -\frac{a_l}{4}[Q^{(m)}_l(t) - Q^{(n)}_l(t)]^2 - \frac{1}{4\hbar^2 a_l}[P^{(m)}_l(t) - P^{(n)}_l(t)]^2 + \frac{i}{2\hbar}[Q^{(m)}_l(t) - Q^{(n)}_l(t)][P^{(m)}_l(t) + P^{(n)}_l(t)] \right\}$$

$$J^{(mn)}_{\text{phase}}(t) = \exp\left\{ -\frac{i}{\hbar}\int_0^t \mathrm{d}\tau\, [L_m(\tau) - L_n(\tau)] \right\}$$

$$= \exp\left\{ -\frac{i}{\hbar}\int_0^t \mathrm{d}\tau\, [\Delta K^{(mn)}(\tau) - \Delta\epsilon^{(m)}_{mn}(\tau) - \Delta\epsilon^{(mn)}_n(\tau)] \right\} \quad (52)$$

where $\Delta K^{(mn)}(t) = K^{(m)}(t) - K^{(n)}(t)$ is the difference in kinetic energies between trajectories propagated on the m th and n th surfaces, respectively, and $\Delta\epsilon^{(mn)}_n(t) = \epsilon^{(m)}_n[\mathbf{Q}(t)] - \epsilon^{(n)}_n[\mathbf{Q}(t)]$. Note that $\epsilon^{(m)}_m[\mathbf{Q}(t)] - \epsilon^{(n)}_n[\mathbf{Q}(t)] = \Delta\epsilon^{(m)}_{mn}(t) + \Delta\epsilon^{(mn)}_n(t)$ has been used, where the $\Delta\epsilon^{(mn)}_n(t)$ term has apparently been omitted by Prezhdo and Rossky.[62]

With eq 52 plugged into the rate expression eq 50, a quantum/semiclassical approximation to the quantum Golden Rule rate is obtained. Staib and Borgis, on the other hand, have obtained the quantum/classical rate expression[65]

$$w^{(qc)}_{m\to n} = \frac{1}{\hbar^2}\int_{-\infty}^{+\infty} \mathrm{d}t \left\langle V^{(qc)}_{mn}(t) V^{(qc)}_{nm}(0) \exp\left\{\frac{i}{\hbar}\int_0^t \mathrm{d}\tau\, \Delta\epsilon^{(m)}_{mn}(\tau)\right\}\right\rangle_{\mathrm{B}} \quad (53)$$

The difference between eqs 50 and 53 is conveniently expressed as[62]

$$J^{(mn)}(t) = \exp\left\{\frac{i}{\hbar}\int_0^t \mathrm{d}\tau\, \Delta\epsilon^{(m)}_{mn}(\tau)\right\} D^{(mn)}(t)$$

$$D^{(mn)}(t) = J^{(mn)}_{\text{overlap}}(t) \exp\left\{ -\frac{i}{\hbar}\int_0^t \mathrm{d}\tau\, [\Delta K^{(mn)}(\tau) - \Delta\epsilon^{(mn)}_n(\tau)] \right\} \quad (54)$$

in terms of the decoherence function $D^{(mn)}(t)$, such that

$$w^{(qm)}_{m\to n} \cong \frac{1}{\hbar^2}\int_{-\infty}^{+\infty} \mathrm{d}t \left\langle V^{(qc)}_{mn}(t) V^{(qc)}_{nm}(0) \exp\left\{\frac{i}{\hbar}\int_0^t \mathrm{d}\tau\, \Delta\epsilon^{(m)}_{mn}(\tau)\right\} D^{(mn)}(t)\right\rangle_{\mathrm{B}} \quad (55)$$

In other words, the quantum/classical rate formula of eq 53 takes into account only part of the overlap $J^{(mn)}(t)$, namely a quantum/classical part of the phase term $J^{(mn)}_{\text{phase}}(t)$ (eq 52), while the rate expression of eq 55 provides a quantum/semiclassical correction in terms of the decoherence function $D^{(mn)}(t)$ (eq 54), most notably determined by the nuclear overlap $J^{(mn)}_{\text{overlap}}(t)$ (eq 52) of two frozen Gaussian wave functions evolving on the two nonadiabatically coupled surfaces $\epsilon_m[\mathbf{Q}(t)]$ and $\epsilon_n[\mathbf{Q}(t)]$, respectively.

Obviously, if the forces experienced by the classical degrees of freedom strongly depend on the adiabatic state of the quantum subsystem, the nuclear overlap contained in the decoherence function will decay quickly as the trajectories $\{\mathbf{Q}^{(m)}(t),\mathbf{P}^{(m)}(t)\}$ and $\{\mathbf{Q}^{(n)}(t),\mathbf{P}^{(n)}(t)\}$ diverge. This is typically the case for electronically nonadiabatic processes in large molecules and condensed phases. If, however, the forces exerted on the classical DoF happen to be almost insensitive to the adiabatic quantum state, the decoherence function will stay close to unity, $D^{(mn)}(t) \cong 1$, and the quantum/semiclassical rate expression of eq 55 practically converges to the quantum/classical limit eq 53. The latter naturally includes quantum/classical pure dephasing effects through its phase factor, as mentioned above. Since, however, both quantum/classical pure dephasing and quantum decoherence effects crucially depend on topological differences between potential surfaces, they are closely related and therefore not independent of one another.

When our nonadiabatic couplings $V^{(qc)}_{mn}(t) = -i\hbar\, \mathbf{d}_{mn}[\mathbf{Q}(t)]\cdot\dot{\mathbf{Q}}(t)$ of eqs 35−36 and $\Delta\epsilon^{(m)}_{mn}(t) = \hbar\omega_{mn} = \hbar\omega_0(m-n)$ (eq 32) are substituted into the quantum/classical rate formula (eq 53), with additional account of quantum/classical energy balance, we immediately obtain our rate expression of eq 40 (assuming stationarity of the bath force $F(t)$ and its time derivative). Quantum/classical pure dephasing effects are rigorously absent due to the fact that the bare adiabatic energy surfaces $\epsilon_m[\mathbf{Q}(t)]$ (eq 32) all experience the same time-dependent vertical shift by a displacement of the classical degrees of freedom. Moreover, this also implies that the forces (eq 34) on the classical DoF due not depend on the adiabatic state of the quantum oscillator. The decoherence function is therefore $D^{(mn)}(t) \equiv 1$ rigorously. Trajectories evolving on different adiabatic surfaces from the same initial conditions due not diverge; thus, $J^{(mn)}_{\text{overlap}}(t) = 1$ (eq 52), and also $\Delta K^{(mn)}(t) = 0$ and $\Delta\epsilon^{(mn)}_n(t) = 0$ (eq 54). Thus, both quantum/classical pure dephasing and quantum/semiclassical decoherence effects in the adiabatic basis are rigorously absent for our present model, as to be expected for a perfectly harmonic system. The simultaneous absence of both effects should also not come as a surprise due to their close relationship.

As a result, the phase factor $\mathrm{e}^{i\omega_{mn}t}$, contained in the quantum/classical rate expression eq 53, is the only factor out of the semiclassical expression for the overlap $J^{(mn)}(t)$ (eqs 52 and 54) that survives. This justifies the neglect of genuine quantum decoherence effects in the vibrationally adiabatic energy basis for the present model and the use of quantum/classical rate expressions eqs 40 and 53. What remains to be considered is dephasing due to energy relaxation, operating on a longer time scale. This effect has been included in our "hopping with complete dephasing" implementation of TFS−SH. As noted above, it takes into account the stochastic interruption of coherent evolution by quantum transitions, repreparing the subsystem in a new quantum state, and ensures that the ensemble averaged transition rates $w_{m\to n}$ are consistent with the occupied state m in the Markovian limit. The latter component of decoherence/dephasing, which is always present in dissipative systems due to relaxation of energy level populations, but is usually neglected in quantum/classical simulations, has been shown in previous subsections to be important for establishing quantum detailed balance in surface hopping simulations of vibrational energy relaxation.

3.2.5. Detailed Balance: Numerical Evidence and Theoretical Arguments. While the previous discussion served to justify our "hopping with complete dephasing" implementation of TFS−TSH and the use of quantum/classical rate expressions, eqs 40 and 53, it is not a priori self-evident that the momentum adjustment along the nonadiabatic coupling vector accompanying a successful hop and the associated existence of rejected hops automatically guarantee quantum detailed balance. Here, we provide additional (numerical) support for quantum detailed balance being (approximately) obeyed by our modified TFS−SH scheme, and show how the statistics of frustrated hopping is related to it, provided that additional requirements are met. In surface hopping quantum/classical dynamics the detailed balance relation $w_{m\to n}/w_{n\to m} = \mathrm{e}^{-\beta\hbar\omega_{mn}}$ (if applicable) for any pair of transitions $m\to n$ and $n\to m$ ($n > m$) can only be achieved through the rejected hopping "cutoff" (eq 42), operating exclusively on the upward transition ($m \to n$). During simulations, the number of transitions $m \to m \pm 1$ (N_{up}, N_{down}) as well as the number of rejected hops (N_{rejected}) has been counted at each time step, such that $N_{\mathrm{up}}(t) + N_{\mathrm{rejected}}(t)$ is the number of $m \to m + 1$ transitions attempted. Consequently, the statistical ratio $p_{m+1}/p_m = \bar{n}/(\bar{n} + 1) = \mathrm{e}^{-\beta\hbar\omega_0}$ at thermal equilibrium (provided that quantum detailed balance applies) should be related to frustrated hopping statistics through

$$\frac{\langle N_{\mathrm{rejected}}(t)\rangle}{\langle N_{\mathrm{up}}(t)\rangle + \langle N_{\mathrm{rejected}}(t)\rangle} = 1 - \mathrm{e}^{-\beta\hbar\omega_0} \qquad (56)$$

where the fraction of rejected hops is a measure of that part of the classical phase space density which does not facilitate upward transitions $m \to m + 1$ in the quantum subsystem, due to quantum/classical energy conservation restrictions. The same should also approximately hold true for the time-integrated quantitities $\int_0^\tau \mathrm{d}t\langle N(t)\rangle/\tau$. Figure 6b shows that this is the case (for TFS−TSH with dephasing), where the ensemble averaged data have been additionally averaged over time windows of 200 *fs*. The statistics derived from $\langle N_{\mathrm{up}}(t)\rangle$ and $\langle N_{\mathrm{rejected}}(t)\rangle$ is not satisfactory, but from the time-integrated data we judge that detailed balance is only approximately obeyed. The theoretical frustrated hopping fraction as derived from detailed balance is $1 - \mathrm{e}^{-\beta\hbar\omega_0} \cong 0.698$ for $\omega_0/2\pi c = 250\ \mathrm{cm}^{-1}$ and $T = 300$ K. Working backward from the numerical data (time-integrated quantities), we would obtain $\omega_{\mathrm{eff}}/2\pi c \simeq 225 \pm 31\ \mathrm{cm}^{-1}$. This means that our above analysis of the approach to thermal equilibrium, based on the oscillator frequency $\omega_0/2\pi c = 250\ \mathrm{cm}^{-1}$, is not perfectly sound, but a reanalysis is skipped here because it gives only minor corrections.

Interestingly, without dephasing we observe (Figure 6a) that the fraction of rejected hops is typically larger, i.e., $1 - \mathrm{e}^{-\beta\hbar\omega_{\mathrm{eff}}} > 1 - \mathrm{e}^{-\beta\hbar\omega_0}$, giving an effective oscillator frequency $\omega_{\mathrm{eff}}/2\pi c \simeq 272 \pm 39\ \mathrm{cm}^{-1}$. Although, within the limits of numerical accuracy, the frustrated hopping fraction of Figure 6a seems to suggest that quantum detailed balance is approximately obeyed also without dephasing, we have strong reasons to believe (Figure 3a) that the oscillator relaxes to a quasi-classical rather than a quantum statistical equilibrium. A resolution of this apparent contradiction may be seen by inspection of the quantum/classical rate expression eq 40 and its derivation, eqs 37−40, from the TSH transition probabilities (eqs 5−7). Equation 37 for the single-trajectory vibrational coherences $\rho_{mn}(t)$, at short times $t \geq t_{\mathrm{hop}}$ after the preceding surface hop ($t_{\mathrm{hop}} = 0$), can only be valid if $\rho_{mn}(t_{\mathrm{hop}}) = 0$ (or approximately so). For our "hopping with complete dephasing" modification of TFS−SH this is the case. Specifically, $\rho_{nn}(t_{\mathrm{hop}}) = \delta_{mn}$, i.e.,

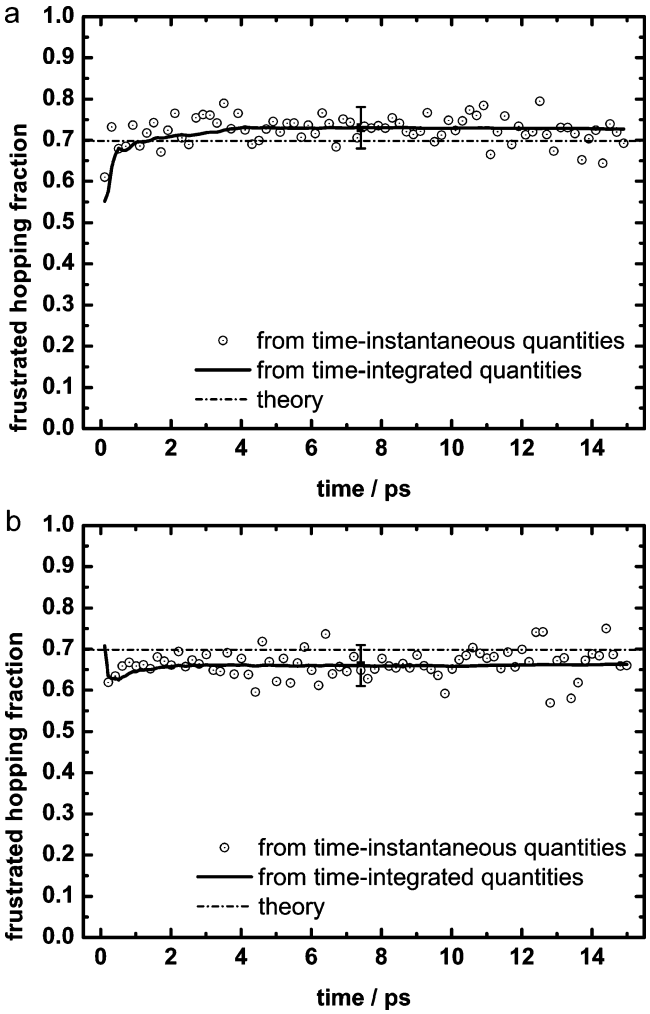

Figure 6. Frustrated hopping fraction $\langle N_{\mathrm{rejected}}(t)\rangle/\{\langle N_{\mathrm{up}}(t)\rangle + \langle N_{\mathrm{rejected}}(t)\rangle\}$ computed from time-instantaneous and time-integrated quantities, respectively (see text), as compared to the theoretical detailed balance prediction, $1 - \mathrm{e}^{-\beta\hbar\omega_0} \cong 0.698$, for a: the original, and b: our modified TFS−TSH. Numerical data points with error bar serve to indicate the respective overall statistical uncertainties (<10%).

the coherences and populations at $t \geq t_{\mathrm{hop}}$ are *causally connected* to (originate from) the pure adiabatic state $|m\rangle$, the currently occupied state. Without dephasing, eq 37 must be replaced by

$$\rho_{mn}(t) = -\sum_{k\neq m}\int_{t_0}^{t}\mathrm{d}t'\ \mathrm{e}^{-i\omega_{mn}(t-t')}\,\mathbf{d}_{mk}\cdot\dot{\mathbf{Q}}(t')\,\rho_{kn}(t') + \sum_{k\neq n}\int_{t_0}^{t}\mathrm{d}t'\ \mathrm{e}^{-i\omega_{mn}(t-t')}\,\rho_{mk}(t')\,\mathbf{d}_{kn}\cdot\dot{\mathbf{Q}}(t') \qquad (57)$$

with the integrals now runnning over the full time range of simulations starting at $t_0 = 0$, where $\rho_{nn}(t_0) = \delta_{m_0,n}$ and $\rho_{mn}(t_0) = 0$, and all coherences and populations evolving from this initial state up to time t have in principle to be taken into account. This makes it difficult to relate the Pauli rate coefficients $w_{m\to n} = \langle p_{m\to n}(t;\delta t)\rangle/\delta t$ (eq 11), obtained via surface hopping probabilities of eq 7, to quantum/classical Golden Rule rate theory (eqs 21, 22, 38−40, and 46). In particular, we have observed (Figures 2a, 3a) that the original TFS−SH scheme implies comparatively large coherences $\rho_{mn}(t) = a_m(t)a_n^*(t)$ of the currently occupied vibrationally adiabatic state $m(t)$ with higher energy states $n > m$, and an undue bias toward upward transitions $m \to m + 1$ on the single-trajectory level. Although the quantum/classical energy balance provides an overall "thermodynamic cutoff" for upward transitions, reflected by the

frustrated hopping fraction (eq 56), the single-trajectory coherences (eq 57) are not causally connected to the *currently occupied* state $|m\rangle$ but originate from the *initial* adiabatic state $|m_0\rangle$. It is therefore argued that quantum/classical energy conservation, as reflected by the frustrated hopping fraction for transitions $m \rightarrow m + 1$, is in general a necessary but *not sufficient* condition for establishing detailed balance in the quantum subsystem. A second requirement is the consistency of single-trajectory coherences and populations with the occupied state index $m(t)$, such that the transition events $k \rightarrow n$ and $n \rightarrow k$ are causally connected to states $|k\rangle$ and $|n\rangle$, respectively. Again, this underscores the significance of introducing, at the single-trajectory level, a mechanism of dephasing as related to population relaxation, but leaves open the question, why the original TFS−SH scheme specifically seems to entail relaxation of the subsystem oscillator toward a quasi-classical thermal equilibrium. The latter issue surely deserves further consideration.

For the sake of comparison with the results of Parandekar and Tully,[41] we note that the case of a quantum two-level system $\{|0\rangle,|1\rangle\}$ corresponds to a special situation, where eq 57 naturally reduces (exactly) to eq 37

$$\rho_{10}(t) = -\int_{t_0}^{t} dt'\, e^{-i\omega_{10}(t-t')}\, \mathbf{d}_{10}\cdot\dot{\mathbf{Q}}(t')\{\rho_{00}(t') - \rho_{11}(t')\} \quad (58)$$

leading to TFS−TSH Golden Rule rate coefficients (cf. eq 40)

$$w_{m\rightarrow n} = \left\langle \frac{2\mathrm{Re}\{\mathbf{d}_{mn}\cdot\dot{\mathbf{Q}}((t)\ \rho_{nm}(t)\}}{\rho_{mm}(t)} \right\rangle_{m\rightarrow n} \simeq \int_{-\infty}^{+\infty} d\tau\, e^{-i\omega_{nm}\tau} \langle \mathbf{d}_{mn}\cdot\dot{\mathbf{Q}}(\tau)\, \mathbf{d}^{*}_{mn}\cdot\dot{\mathbf{Q}}(0)\rangle_{m\rightarrow n} \quad (59)$$

with $m = 1$ (0) and $n = 0$ (1), and the subscript $m \rightarrow n$ as a reminder for observing quantum/classical energy conservation constraints. Although the coherences at time t originate from $|m_0\rangle$ at $t = t_0$, and not from $|m\rangle$ at $t = t_{\mathrm{hop}}$, quantum detailed balance may still be maintained, as argued shortly below, since the single-trajectory quantum reference populations $\rho_{nn}(t) = |a_n(t)|^2$, not the occupied state populations $p_n(t) = \delta_{n,m(t)}$, (rapidly) *cycle* between states $n = 0, 1$. An important similarity of our present model of vibrational energy relaxation and the two-state model of Parandekar and Tully[41] is the constancy in time of the nonadiabatic coupling vector (cf. eq 35). In both cases the quantum subsystem is continuously driven by an external (generalized) force. The essential difference between the above two-state model and our present model situation is the latter's multilevel feature. As observed by Parandekar and Tully,[41] the ensemble averaged squared quantum amplitudes reflect a uniform distribution, $\langle|a_0|^2\rangle = \langle|a_1|^2\rangle = 0.5$, at asymptotic equilibrium, while the asymptotic ensemble averaged occupied state populations are in accord with a quantum statistical equilibrium (quantum detailed balance) at specified finite bath temperature, $\langle p_1\rangle/\langle p_0\rangle = e^{-\beta\hbar\omega_{10}}$. The authors note that the discrepancy between (single-trajectory or ensemble averaged) quantum reference and occupied state populations, $\rho_{nn}(t)$ and $p_n(t)$, respectively is an essential requirement (or consequence) of TFS−SH, because quantum detailed balance is achieved through the appearance of frustrated hops (by imposing quantum/classical energy balance). Without frustrated hopping, $\langle p_n(t)\rangle \cong \langle\rho_{nn}(t)\rangle$, and the quantum two-level system would approach infinite temperature. On this part, we fully agree.

Moreover, Parandekar and Tully (seem to) claim that frustrated hopping, leading to the discrepancy between $\langle\rho_{nn}\rangle$ and $\langle p_n\rangle$, is a necessary and *sufficient* feature of the original TFS−TSH scheme for obtaining quantum Boltzmann populations at long times in a general multilevel quantum subsystem. On this part we disagree. As shown for our damped harmonic oscillator case (Figures 2a and 3a), the original TFS−SH scheme entails relaxation of the excited quantum oscillator (in terms of occupied state populations), but not toward a quantum statistical equilibrium. As implicit in the evolution of the mean adiabatic occupation number $\langle\hat{n}_{\mathrm{ad}}\rangle_t$ (Figures 2a and 3a), quantum amplitude $a_n(t)$ leaks out into states $m_0 \pm 1$, $m_0 \pm 2$, etc. successively accessible from the *initially* occupied adiabatic state m_0. No state other than $m_0 = 5$ may attain a quantum reference population close to unity, $\rho_{nn}(t) \cong 1$, at later times (not shown here, but cf. ref 34), just as a consequence of the unitary time-reversible Schrödinger dynamics. Such an event of state vector recurrence to $|\Psi_S(t)\rangle \cong |\Psi_S(0)\rangle = |m_0\rangle$ is actually contained in the single-trajectory sample of Figure 2a ($\langle\hat{n}_{\mathrm{ad}}\rangle_t \cong m_0 = 5$), with observable consequences for the evolution of the occupied state $m(t)$ (see below). Thus, the single-trajectory quantum amplitudes of the original TFS−SH generally cannot in any way be interpreted as having evolved from an initial state other than $|m_0\rangle$. This is in contrast to the special case of a two-level system, where the quantum amplitude merely *cycles* between *two* states. For our modified TFS−TSH scheme (Figures 2b, 3b), there *is* a discrepancy between the expectation value $\langle\hat{n}_{\mathrm{ad}}\rangle_t$ and the occupied state index $m(t)$ ($\rho_{mm}(t)$ and $p_m(t)$) and their ensemble averaged values, but it is kept *minimal*. During unitary quantum evolution between surface hops amplitude spreads into neighboring states of the *currently* occupied adiabatic state m, prepared in the preceding hop through our "hopping with complete dephasing". No adiabatic state other than m (state vector revival) may acquire a quantum reference population close to unity. The range of states with significant quantum amplitude is usually dominated by the currently occupied state and includes those states which are *directly* accessible from the latter ($n = m \pm 1$ via matrix elements q_{mn}). In contrast, when using the original TFS−SH scheme the currently occupied state and its neighbors may be contained in the small-amplitude tail of the quantum superposition $|\Psi_S(t)\rangle = \sum_n a_n(t)|n\rangle$. In this typical rather than exceptional case, during single-trajectory evolution the occupied state index $m(t)$ will consequently be forced to evolve toward the large-amplitude center of the superposition. With $|m_0\rangle$ being an energetically excited state, the center of the quantum superposition evolves toward higher energy states ($\langle\hat{n}_{\mathrm{ad}}\rangle_t \geq m_0$), while the occupied state index is more likely to evolve toward lower energy states (quantum/classical energy balance), placing the currently occupied state $m(t)$ in the lower energy tail of $|\Psi_S(t)\rangle$. State vector revivals, full or partial, offer an observable signature of the occupied state being pushed back toward the (higher energy) center of the quantum superposition (undue bias toward upward transitions), if permitted by the energy conservation constraint. Such signatures are clearly visible in Figure 2a, including a full recurrence and at least two partial (attempted) ones. We believe that this phenomenon is at the heart of our observation that the original TFS−TSH scheme fails to reproduce quantum detailed balance even approximately for our present model, as an example of a general multilevel quantum subsystem. Again, a two-level system contains by definition only two states which are *directly* accessible from each other, one of which may be the currently occupied one. It appears practically unimportant, from which of the two possible initial states, $m_0 = 0$ or 1, the current single-trajectory coherences and populations have evolved. Both states may attain a quantum reference population $\rho_{nn}(t) = 1$. In fact,

the quantum amplitudes at time t may equally well have emerged from either initial state, just as a result of time-reversal symmetry. Tully's original and our modified TFS−TSH scheme are therefore expected to give the same results; i.e., the "hopping with complete dephasing" modification appears unnecessary, in the case of a quantum two-state system.

In summary, the above arguments are just another variant of our theme saying that, in addition to observing the quantum/classical energy balance during hopping, the *single-trajectory* quantum reference state $|\Psi_S(t)\rangle$ should be consistent with (causally connected to) the currently occupied state $m(t)$, to obtain meaningful TFS−SH rate coefficients and reproduce quantum detailed balance in a general multilevel quantum subsystem.

To complete our discussion of Parandekar and Tully's work,[41] we just add two remarks related to the *dynamics* of approach to a quantum thermal equilibrium. First, the authors conclude that the attainment of a quantum statistical equilibrium depends (crucially?) on the fact that their quantum two-state variables $X = |a_1|^2 = 1 - |a_0|^2$ and $Y = a_0 a_1^* + a_1 a_0^*$ are statistically separable from the classical momentum (of the chain atom directly coupled to the quantum subsystem in their model), i.e., classical momentum and quantum amplitudes are uncorrelated. In light of Golden Rule rate theory (eqs 58 and 59), it appears to us that this may not be quite right. In fact, eq 58 (eq 37) shows that (single-trajectory) coherences and bath momenta are dynamically correlated, such that the coherences can be eliminated from the equations of motion, when focusing on the population dynamics within second-order perturbation theory for the subsystem density operator. On the ensemble level, the coherences may be considered irrelevant (in the sense of coarse-graining as implied by a Pauli master equation), but still the statistics of coherences should be related to the statistical properties of bath momenta. Second, as a corollary, from the TFS−SH transition/hopping probabilities (eqs 5−7; cf. eq 59) being proportional to quantum coherences and classical momenta (projected onto the nonadiabatic coupling vector) it follows by way of eq 58 that, within Golden Rule rate theory, the hopping rate coefficients $w_{m\to n}$ are related to (the Fourier transform of) a *correlation function* of projected bath momenta (eq 59; see also eqs 50, 53, and 55). Thus, the hopping rate coefficient (eq 59) contains the dynamical correlation between quantum coherences and classical bath momenta in terms of a (projected) momentum correlation function. Altogether, the above comments on Parandekar and Tully's important work are not meant as harsh criticism (or hair-splitting), but rather as a complementary rate theoretical view on the TFS−TSH method and its ability to describe the approach to thermal equilibrium of an intrinsically multilevel quantum subsystem.

3.3. Discussion. We have investigated the statistical mechanical properties of Tully's fewest switches surface hopping method for the model of a linearly damped harmonic oscillator. In its original version, TFS−SH was shown to fail in producing an asymptotic quantum statistical thermal mixture of vibrationally adiabatic states. Instead, a quasi-classical asymptotic thermal distribution is observed. While the numerical frustrated hopping statistics seems to be in accord with quantum detailed balance, the origin of the above failure is traced back to the single-trajectory quantum amplitudes evolving coherently from the initial adiabatic state $|m_0\rangle$ at time $t_0 = 0$, rather than from the currently occupied state $|m\rangle$, prepared in the preceding hop at time t_{hop}. As a remedy, we have suggested resetting the coherently evolving state vector to the new adiabatic state, $|\Psi(t_{\mathrm{hop}})\rangle \to |\chi_n[\mathbf{Q}(t)]\rangle$, during hopping ($m \to n$). This procedure can be motivated by a variety of related arguments, applying to dissipative subsystems as a result of their coupling to a large, effectively thermal environment. First, simple considerations based on a Redfield master equation in the secular limit show that the rates $w_{m\to n}$ of local population relaxation define a minimum rate of dephasing. Second, in a more microscopic description, the rates of escape events $m \to n$ from the currently occupied adiabatic state $|m\rangle$ should, after some short transient period following the preceding hop ($t = t_{\mathrm{hop}}$), become independent of the previous history ($t \le t_{\mathrm{hop}}$) of the stochastically evolving occupied state $m(t)$, and of the underlying single-trajectory adiabatic coherences and populations, determining the hopping statistics for times up to t_{hop} (emergence of Markovian subdynamics). Third, the property of quantum detailed balance, $w_{m\to n}/w_{n\to m} = \mathrm{e}^{-\beta\hbar\omega_{mn}}$ for any pair of states m and n, requires that the surface hopping rate coefficients $w_{m\to n} = \langle p_{m\to n}(t;\delta t)\rangle/\delta t$ and $w_{n\to m}$ are sampled under conditions, that the composite quantum/classical system may be considered as prepared in states $\hat{\rho}_{\mathrm{SB}}(\mathbf{Q},\mathbf{P}) = |m\rangle\rho^{(m)}(\mathbf{Q},\mathbf{P})\langle m|$ and $|n\rangle\rho^{(n)}(\mathbf{Q},\mathbf{P})\langle n|$, respectively, shortly after (or, approximately, immediately at) the preceding hop, where the classical phase space densities are $\rho^{(k)}(\mathbf{Q},\mathbf{P}) \simeq \rho_{\mathrm{eq}}^{(k)}(\mathbf{Q},\mathbf{P})$. For a quantum system immersed in a large heat reservoir (even a nonergodic one), individual non-equilibrium classical environmental trajectories generated by the TFS−SH scheme may for practical purposes indeed be regarded as members of a classical thermal ensemble $\rho_{\mathrm{eq}}^{(m)}(\mathbf{Q},\mathbf{P})$, possibly depending on the occupied state m of the quantum subsystem. Resetting the coherently evolving quantum state vector during hopping, as suggested, then naturally meets, upon ensemble averaging, the above physical requirements. The overall picture of TFS−SH thus suggested is one where both quantum and classical subsystems are affected in a discontinuous manner (apparent "collapse" and momentum adjustment, respectively) during hopping.

Our "hopping with complete dephasing" version of TFS−TSH, which was shown to (approximately) fulfill quantum detailed balance, might be considered a too drastic modification of Tully's original scheme. Indeed, the latter has proven a very useful tool especially for modeling electronically nonadiabatic processes and proton/hydrogen transfer. Keeping at least some degree of coherence across hopping events may, for instance, be necessary for a better description of possible interference effects in the case of successive avoided crossings. On the other hand, the necessity of including decoherence effects has been stressed by quite a number of research groups,[25,29−32,39] and the general notion of quantum decoherence in open system dynamics has by now become widely accepted, even though still subject to debate.[28] In any case, the physical nature of quantum coherences produced by classical external time-dependent fields is different from those generated by quantum system-environment interactions.[66] Quantum system−bath correlations arising from diagonal (in the $\{|n\rangle\}$-space) interactions provide a mechanism for local *decay* of coherence in a subsystem.[27] Classical external driving fields, even if subject to quantum/classical backreaction, generally tend to spread coherence, and thus population, (almost) uniformly across the quantum state space.[34,41] In particular, for vibrationally nonadiabatic transitions we have observed that, when hopping takes place to lower energy states during a single surface hopping trajectory, coherences involving higher energy states are maintained, leading as argued to the above failure of Tully's original SH scheme. Ensemble averaging cannot generally be expected to provide a remedy to this unphysical situation, except maybe for special cases. Without ad hoc inclusion of decoherence/

dephasing effects there is no way to arrive at a rigorous quantum statistical mixture for the ensemble averaged subsystem density operator.

To place the suggested modification of TFS−TSH in a clear general context, we have tried to identify, in a fairly detailed discussion, various mechanisms of decoherence/dephasing as relevant to quantum/classical dynamics simulations. While quantum/classical pure dephasing is naturally included in QCMD methods, genuine quantum decoherence can only approximately be taken into account via quantum/semiclassical corrections. Both are related to topological differences between potential energy surfaces $\epsilon_m[\mathbf{Q}(t)]$ and $\epsilon_n[\mathbf{Q}(t)]$, i.e., sufficiently strong diagonal system-environment interaction, and are rigorously absent in the vibrationally adiabatic basis for the present model situation of a linearly damped harmonic oscillator.

In contrast, dephasing as related to energy/population relaxation is physically distinct from the latter dephasing mechanisms in that it originates from nondiagonal (system−bath) interactions, which drive the energy dissipation. It is therefore present in all dissipative systems and determines the loss of phase coherence at long times. The "hopping with complete dephasing" version of TFS−SH, suggested here for reasons of consistency, corresponds to an extreme version of introducing dephasing due to population relaxation, where the mean time length of adiabatic coherence is given by the average time between nonadiabatic transitions, and coherence is not maintained across hopping between potential surfaces. It essentially restricts TFS−SH to the limit of incoherent hopping between adiabatic states, where the quantum state vector becomes a purely auxiliary quantity for sampling the rate coefficients of a Markovian Pauli master equation during coherent evolution between hopping events. From the algorithmic point of view, it is regarded as a minimal extension of Tully's fewest switches SH, which is expected to reproduce the emergence of Markovian subdynamics and quantum detailed balance, provided that sources of decoherence/dephasing other than population relaxation may be neglected. In special cases, as, e.g., for quantum two-state systems,[41] it may not even be needed. For the linearly damped *anharmonic* oscillator, both quantum/classical pure dephasing and quantum decoherence effects, though possibly weak, are also expected to be relevant.

Condensed phase vibrational energy relaxation (VER), for which we have considered a simple model here, has only recently become the subject of investigation using quantum/classical dynamics methodology,[16−18,33,34,67−69] the exception being the quantum/classical Pauli master equation approach using classical equilibrium force correlation functions[55,56] (see also references in ref 34). The latter has a long history in the field of vibrational energy transfer, but differs from the quantum/classical dynamics methods discussed here:[56] Quantum and classical equations of motion are not solved simultaneously. Instead, classical dynamics is used first to generate the equilibrium fluctuation forces, from which (approximate) quantum transition rates are computed later on. Thus, the applicability of surface hopping or mean field quantum/classical dynamics methods to vibrational energy relaxation, and especially their relation to the more traditional approaches, appear as yet largely unexplored.[56] Vibrational energy relaxation differs from the electronically nonadiabatic case in that, for a single vibrational DoF ("diatomic" VER), avoided level crossings do not appear, and the nonadiabatic coupling region is typically delocalized in the phase space of the classical degrees of freedom.

Our main results are that TFS−TSH, with appropriate inclusion of dephasing, for the linearly damped oscillator (i) reproduces quantum detailed balance, and (ii) gives Oxtoby's quantum prefactor (or correction factor)[55,56] for the overall average rate of energy relaxation. While the first property has recently been obtained by Parandekar and Tully[41] for a two-level quantum system coupled to the first atom of a linear chain, the second property has, to the best of our knowledge, not been recognized before. It implies that fewest switches SH is, at least for the case of dominantly linear dissipation, not superior to the quantum/classical Pauli master equation approach to VER mentioned above, while being computationally much more demanding. In particular, it seems to reproduce one specific quantum prefactor (for the bath force correlation spectrum) out of a variety of possibilities.[70−72] For our present model and parameter situation, the prefactor $f(\omega_0,T)$ for the overall average rate of relaxation, defined through the relation $\bar{w}_{qc} = f(\omega_0,T)\bar{w}_{cl}$, takes the values 0.895, 1.061, and 1.030 when using the standard (Oxtoby), Schofield, and harmonic/Schofield corrections, respectively (cf. ref 72), while the harmonic prefactor is trivially $f(\omega_0,T) = 1$. With our modified TFS−SH scheme, the observed average rate of relaxation $\bar{w}_{qc}$ is definitely smaller than $\bar{w}_{cl} = 0.2\ \mathrm{ps}^{-1}$ ($\tau_{qc} > \tau_{cl}$) and is very well reproduced by the standard correction, $f(\omega_0,T) \simeq 0.895$.

A weakness of our present study is our inability to arrive, in an analytically rigorous way, at the quantum/classical rate expressions reproduced numerically. Rather, we arrived at these rate expressions in a semianalytical, partially heuristic manner, sofar limited to the linearly damped *harmonic* oscillator. We believe that this is an important issue for further investigation. As stated by Berne and co-workers,[56] "it remains an open question, whether those mixed quantum-classical treatments" (including TFS−SH) "agree with our mixed quantum-classical results" (the Oxtoby prefactor) "in the regime where lowest order perturbation theory is valid". Importantly, our combined numerical and analytical study suggests that the validity of quantum detailed balance (with Oxtoby's prefactor) for TFS−TSH in the second-order perturbative regime requires, in addition to frustrated hopping, the inclusion of some kind of state vector "collapse" during single-trajectory hopping. In general, it is expected that the TFS−SH transition rates not only depend on whether decoherence/dephasing is introduced but also depend on which relevant sources of dephasing are taken into account. In this sense, the above question is still open, e.g., for the linearly damped but *anharmonic* oscillator.

As to the issue of quantum decoherence,[26,27] we stress once more that our "hopping with complete dephasing" extension of TFS−TSH is not meant to imply that the adiabatic working basis of the SH scheme be regarded as a pointer basis (in the sense that it dynamically minimizes the coherences via system−bath entanglement), since the underlying mechanism invoked is distinct from genuine quantum decoherence. While for electronically nonadiabatic transitions the diabatic/adiabatic alternative[25] provides relevant candidates for the pointer basis, for quantum nuclear or vibrational (harmonic or anharmonic) motion coherent states (minimum-uncertainty wave packets) are expected to play the role of pointer states.[73−75] Interestingly, coherent states of the quantum harmonic oscillator represent the only type of quantum initial states for which the mean field Ehrenfest method, for (dominantly) linear damping, gives physically reasonable results.[33,34] From a pragmatic point of view, if only the populations of the subsystem density matrix in a certain basis are considered relevant, it seems sufficient to identify for the working basis chosen the most important source(s) of dephasing. For vibrational energy transfer in polyatomic molecules intra- and intermolecular energy transfer pathways

(and combinations thereof) come into play, and level degeneracies and avoided crossings due to intramolecular Fermi resonances are expected. In such systems, the treatment of decoherence/dephasing may be crucial, and the present "hopping with complete dephasing" scheme seems incomplete.

4. Conclusion

Tully's fewest switches surface hopping (TFS−SH) method has been applied to the linearly damped oscillator as a model for condensed phase vibrational energy relaxation. In contrast to the original scheme, dephasing in the adiabatic basis was introduced by resetting the quantum state vector to the new occupied vibrationally adiabatic state after each successful hop. This procedure was motivated by the observed failure of Tully's TFS−TSH in reproducing an asymptotic quantum statistical equilibrium for the subsystem oscillator, and was justified by a variety of related arguments, including reference to the corresponding Redfield master equation in the secular limit, and the microscopic requirements for the emergence of Markovian subdynamics and quantum detailed balance.

Using this "hopping with complete dephasing" scheme, it was shown that fewest switches surface hopping gives a quantum statistical asymptotic thermal equilibrium for the quantum subsystem, where the so-called "frustrated hops" ("classically forbidden transitions") appear crucial for maintaining quantum detailed balance. We observe that, for the linearly damped harmonic oscillator, TFS−SH with dephasing predicts on overall rate of energy relaxation which is very closely reproduced by a quantum/classical Pauli master equation approach, with the rate coefficients obtained via Oxtoby's quantum prefactor.[55,56] The same applies to the detailed pattern of population relaxation. While we believe that the latter correspondence is an important and, as to our knowledge, new finding, the mechanistic origin is not yet completely clear to us. In particular, we were not able to give a rigorous analytical proof, and the general agreement with Oxtoby's quantum/classical rate theory beyond the linearly damped *harmonic* oscillator appears uncertain. However, a detailed comparison to the original TFS−SH scheme using statistical theory suggests that dephasing due to population relaxation (as implied by our apparent "collapse" procedure), in addition to frustrated hopping, is indeed necessary for obtaining quantum detailed balance in TFS−TSH simulations of vibrational energy relaxation, while pure dephasing and genuine quantum decoherence are irrelevant in the adiabatic basis for the present model.

When the results obtained here using vibrationally adiabatic surface hopping are compared to the mean field Ehrenfest (mfE) method as applied to the same physical model, an interesting dichotomy arises: While the (single-trajectory) mfE method, when it works physically reasonably, predicts relaxation toward a quasi-classical thermal equilibrium with the overall rate equal to its classical mechanical expression,[34] TFS−SH (with dephasing) gives a quantum statistical equilibrium, but seemingly only at the expense of shifting the rate of energy relaxation below the classical value. Mean field Ehrenfest is a fully coherent method, whereas surface hopping, even when the quantum amplitudes are propagated coherently throughout, introduces some element of incoherence by adding on top of the mechanical equations of motion the feature of adiabatic population hopping, resembling the stochastic "on-the-fly" realization of a quantum/classical Pauli master equation for the "occupied" adiabatic state.

In fact, our "hopping with complete dephasing" scheme corresponds to the extreme version of simulating incoherent hopping between adiabatic states. The quantum state vector propagated along individual quantum/classical trajectories then becomes a purely auxiliary quantity. Coherences sampled along trajectory segments merely provide information about transition probabilities, but are discarded when hopping to a new adiabatic surface.

Combining both coherent and incoherent dynamical aspects together with quantum detailed balance in one universally applicable (basis-independent) quantum/classical method seems hard to achieve.

Acknowledgment. The author is grateful to Profs. Jörg Schroeder and Dirk Schwarzer, and especially to Dr. Anatole Neufeld and Profs. Evgueni Nikitin and Vyacheslav Vikhrenko, for helpful discussions, and, last but least, to Prof. Jürgen Troe for his support over the years. The revised version of the manuscript has appreciably benefited from the critical comments of two reviewers (although this led to a significant growth in page number), which is explicitly acknowledged here.

References and Notes

(1) (a) Allen, M. P.; Tildesley, D. J. *Computer Simulation of Liquids*; Clarendon Press: Oxford, U.K., 1989. (b) Frenkel, D.; Smit, B. *Understanding Molecular Simulation*; Academic Press: San Diego, CA, 1996.
(2) *Classical and Quantum Dynamics in Condensed Phase Simulations*; Berne, B. J., Ciccotti, G., Coker, D. F., Eds.; World Scientific: Singapore, 1998.
(3) Porter, M. A. *Rep. Prog. Phys.* **2001**, *64*, 1165.
(4) Drukker, K. *J. Comput. Phys.* **1999**, *153*, 225.
(5) *Conical Intersections*; Domcke, W., Yarkony, D. R., Köppel, H., Eds.; World Scientific: Singapore, 2004.
(6) *Computational Methods in Photochemistry*; Kutateladze, A. G., Ed.; Taylor & Francis: Boca Raton, FL, 2005.
(7) Hammes-Schiffer, S. *J. Phys. Chem. A* **1998**, *102*, 10443.
(8) Hammes-Schiffer, S.; Billeter, S. R. *Int. Rev. Phys. Chem.* **2001**, *20*, 591.
(9) Chapman, S. *Adv. Chem. Phys.* **1992**, *82*, 423. See also references therein.
(10) Domcke, W.; Stock, G. *Adv. Chem. Phys.* **1997**, *100*, 1.
(11) Stock, G.; Thoss, M. In ref 5, p 619.
(12) Doltsinis, N. L.; Marx, D. *J. Theor. Comput. Chem.* **2002**, *1*, 319.
(13) Doltsinis, N. L. In *Quantum Simulations of Complex Many-Body Systems: From Theory to Algorithms*, *Lecture Notes*; Grotendorst, J., Marx, D., Muramatsu, A., Eds.; NIC Series 10; NIC: Jülich, Germany, 2002; p 377.
(14) Hack, M. D.; Truhlar, D. G. *J. Phys. Chem. A* **2000**, *104*, 7917.
(15) Nikitin, E. E. *Annu. Rev. Phys. Chem.* **1999**, *50*, 1.
(16) Herman M. F. *Int. J. Quantum Chem.* **1998**, *70*, 897.
(17) (a) Thompson, W. H. *J. Chem. Phys.* **2003**, *118*, 1059. (b) Li, S. M.; Thompson, W. H. *J. Phys. Chem. A* **2003**, *107*, 8696.
(18) Batisda, A.; Cruz, C.; Zuniga, J.; Requena, A. *J. Chem. Phys.* **2004**, *121*, 10611.
(19) (a) Tully, J. C. In *Modern Methods for Multidimensional Dynamics Computations in Chemistry*; Thompson, D. L., Ed.; World Scientific: Singapore, 1998; p 34. (b) *Faraday Discuss.* **1998**, *110*, 407.
(20) Jasper, A. W.; Zhu, C.; Nangia, S.; Truhlar, D. G. *Faraday Discuss.* **2004**, *127*, 1.
(21) Donoso, A.; Martens, C. C. *Int. J. Quantum Chem.* **2002**, *90*, 1348.
(22) Micha, D. A.; Thorndyke, B. *Adv. Quantum Chem.* **2004**, *47*, 293.
(23) Horenko, I.; Salzmann, C.; Schmidt, B.; Schütte, C. *J. Chem. Phys.* **2002**, *117*, 11075.
(24) Sergi, A.; Kernan, D. M.; Ciccotti, G.; Kapral, R. *Theor. Chem. Acc.* **2003**, *110*, 49.
(25) Zhu, C.; Jasper, A. W.; Truhlar, D. G. *J. Chem. Theor. Comput.* **2005**, *1*, 527.
(26) Giulini, D.; Joos, E.; Kiefer, C.; Kupsch, J.; Stamatescu, I.-O.; Zeh, H. D. *Decoherence and the Appearance of a Classical World in Quantum Theory*; Springer: Berlin, 1996.
(27) Zurek, W. H. *Rev. Mod. Phys.* **2003**, *75*, 715.
(28) Schlosshauer, M. *Rev. Mod. Phys.* **2004**, *76*, 1267.
(29) Bittner, E. R.; Rossky, P. J. *J. Chem. Phys.* **1995**, *103*, 8130.
(30) Bittner, E. R.; Rossky, P. J. *J. Chem. Phys.* **1997**, *107*, 8611.
(31) Rossky, P. J. In ref 2, p 515.
(32) Prezhdo, O. V. *J. Chem. Phys.* **1999**, *111*, 8366. Prezhdo, O. V.; Brooksby, C. *J. Mol. Struct. (THEOCHEM)* **2003**, *630*, 45.
(33) Käb, G. *Phys. Rev. E*, **2002**, *66*, 046117.
(34) Käb, G. *J. Phys. Chem. A* **2004**, *108*, 8866.
(35) Tully, J. C. *J. Chem. Phys.* **1990**, *93*, 1061.

(36) Hammes-Schiffer, S.; Tully, J. C. *J. Chem. Phys.* **1994**, *101*, 4657.
(37) Coker, D. F.; Xiao, L. *J. Chem. Phys.* **1995**, *102*, 496.
(38) Müller, U.; Stock, G. *J. Chem. Phys.* **1997**, *107*, 6230.
(39) Fang, J.-Y.; Hammes-Schiffer, S. *J. Phys. Chem. A* **1999**, *103*, 9399.
(40) Prezhdo, O. V.; Rossky, P. J. *J. Chem. Phys.* **1997**, *107*, 825.
(41) Parandekar, P. V.; Tully, J. C. *J. Chem. Phys.* **2005**, *122*, 094102.
(42) Kohen, D.; Stillinger, F. H.; Tully, J. C. *J. Chem. Phys.* **1998**, *109*, 4713.
(43) Nettesheim, P.; Bornemann, F. A.; Schmidt, B.; Schütte, C. *Chem. Phys. Lett.* **1996**, *256*, 581.
(44) Bornemann, F. A.; Nettesheim, P.; Schütte, C. *J. Chem. Phys.* **1996**, *105*, 1074.
(45) Jiang, H.; Zhao, X. S. *J. Chem. Phys.* **2000**, *113*, 930.
(46) Blum, K. *Density Matrix Theory and Applicatations*; Plenum: New York, 1981.
(47) Hänggi, P.; Talkner, P.; Borkovec, M. *Rev. Mod. Phys.* **1990**, *62*, 251.
(48) Zwanzig, R. *Nonequilibrium Statistical Mechanics*; Oxford University Press: Oxford, U.K., 2001.
(49) Zwanzig, R. *J. Stat. Phys.* **1973**, *9*, 215.
(50) Caldeira, A. O.; Leggett, A. J. *Ann. Phys. (N.Y.)* **1983**, *149*, 374. Caldeira, A. O.; Leggett, A. J. *Ann. Phys. (N.Y.)* **1984**, *153*, 445 (erratum).
(51) Kubo, R. *Rep. Prog. Phys.* **1966**, *29*, 255.
(52) Hänggi, P.; Ingold, G.-L. *Chaos* **2005**, *15*, 026105.
(53) May, V.; Kühn, O. *Charge and Energy Transfer Dynamics in Molecular Systems*; Wiley-VCH: Berlin, 2000.
(54) Redfield, A. G. *Adv. Magn. Reson.* **1965**, *1*, 1.
(55) Oxtoby, D. W. *Adv. Chem. Phys.* **1981**, *47*, 487.
(56) Egorov, S. A.; Rabani, E.; Berne, B. J. *J. Phys. Chem. B* **1999**, *103*, 10978.
(57) Weiss, U. *Quantum Dissipative Systems*; World Scientific: Singapore, 1993.
(58) Karrlein, R.; Grabert, H. *Phys. Rev. E* **1997**, *55*, 153.
(59) Gardiner, C. W.; Zoller, P. *Quantum Noise*; Springer: Berlin, 2000.
(60) Kubo, R.; Toda, M.; Hashitsume, N. *Statistical Physics II*; Springer: Berlin, 1992.
(61) Egorov, S. A.; Berne, B. J. *J. Chem. Phys.* **1997**, *107*, 6050.
(62) Prezhdo, O. V.; Rossky, P. J. *J. Chem. Phys.* **1997**, *107*, 5863.
(63) Neria, E.; Nitzan, A. *J. Chem. Phys.* **1993**, *99*, 1109.
(64) Heller, E. J. in: *The Physics and Chemistry of Wave Packets*; Yeazell, J., Uzer, T., Eds.; Wiley: Chichester, U.K., 2000; p 31.
(65) Staib, A.; Borgis, D. *J. Chem. Phys.* **1995**, *103*, 2642.
(66) Neufeld, A. A.; Schwarzer, D.; Schroeder, J.; Troe, J. *J. Chem. Phys.* **2003**, *119*, 2502.
(67) Okazaki, S. *Adv. Chem. Phys.* **2001**, *118*, 191.
(68) Terashima, T.; Shiga, M.; Okazaki, S. *J. Chem. Phys.* **2001**, *114*, 5663.
(69) (a) Mavri, J.; Lensink, M.; Berendsen, H. J. C. *Mol. Phys.* **1994**, *82*, 1249. (b) Mavri, J.; Berendsen, H. J. C. *Phys. Rev. E* **1994**, *50*, 198. (c) Berendsen, H. J. C.; Mavri, J. *Int. J. Quantum Chem.* **1996**, *57*, 975. (d) Mavri, J. *Mol. Sim.* **2000**, *23*, 389.
(70) Egorov, S. A.; Skinner, J. L. *Chem. Phys. Lett.* **1998**, *293*, 469.
(71) Skinner, J. L.; Everitt, K. F.; Egorov, S. A. In *Ultrafast Infrared and Raman Spectroscopy*; Fayer, M. D., Ed.; Marcel-Dekker: New York 2001; p 675.
(72) Shi, Q.; Geva, E. *J. Phys. Chem. A* **2003**, *107*, 9059.
(73) Zurek, W. H.; Habib, S.; Paz, J. P. *Phys. Rev. Lett.* **1993**, *70*, 1187.
(74) Tegmark, M.; Shapiro, H. S. *Phys. Rev. E* **1994** *50*, 2538.
(75) Dutra, S. M. *J. Mod. Opt.* **1998**, *45*, 759.